理 學 博 士 學 位 論 文

Polymeric Sensor and Actuators; Synthesis and Characterization of Thiosemicarbazone-based Polymers

蔚 山 大 學 敎 大 學 院

化 學 科

朴 在 民

Polymeric Sensor and Actuators; Synthesis and Characterization of Thiosemicarbazone-based Polymers

指 導 敎 授 **이 형 일**

이 論文**을** 理學博士 學位論文**으로** 提出**함**

2018年 **11**月

蔚 山 大 學 敎 大 學 院

化 學 科

朴 在 民

朴 在 民**의** 理學博士 學位論文**을** 認准**함**

審査委員　　이 승 구 印

審査委員　　정 한 모 印

審査委員　　우 상 국 印

審査委員　　박 종 남 印

審査委員　　이 형 일 印

蔚 山 大 學 敎 大 學 院

2018年 **11**月

Contents

LIST OF ABBREVIATIONS

AIBN : 2,2′-Azobis(Isobutyronitrile)

AFM : Atomic Force Microscope

CTA : Chain Transfer Agent

CMC : Critical Micelle Concentration

DMA : N,N-Dimethylacrylamide

DMP : 2-(Dodecylthiocarbonothioylthio)-2-Methylpropionic Acid

DMF : N,N-Dimethylformamide

DLS : Dynamic Light Scattering

GPC : Gel Permeation Chromatography

ICP-OES : Inductively Coupled Plasma Optical Emission Spectroscopy

LCST : Lower Critical Solution Temperature

NMR : Nuclear Magnetic Resonance

Pnipam : Poly(N-Isopropylacrylamide)

RAFT : Reversible Addition-Fragmentation Chain Transfer

THF : Tetrahydrofuran

VBA : 3-Vinylbenzaldehyde

CCMs : Core-Cross-Linked Micelles

Chapter 1

General Introduction

1. Introduction

The Host-guest chemistry is a widespread, generally occurring important event in nature or human body. The Host-guest chemistry between two or more molecules occurs when they are chemically, geometrically and structurally. In nature, the processes take place in aqueous and are usually involved macromolecules or complex and organized systems. These interactions are extremely specific, and the host (receptor) can be used to develop technological devices, such as membranes, catalysts and sensors.

There is a strong need to combine the host-guest chemistry with a transducing element to develop practically applicable sensing system capable of rapidly detecting chemicals. Thus, if the host-guest recognition phenomenon gives rise to a variation in a macroscopically measurable property, the term sensing can be used; a sensing molecule is a chemical structure capable of eliciting a response that quantifies the presence of an analyte (i.e., a chemical system, or host), which displays an observable response upon selective interaction with a target(guest).

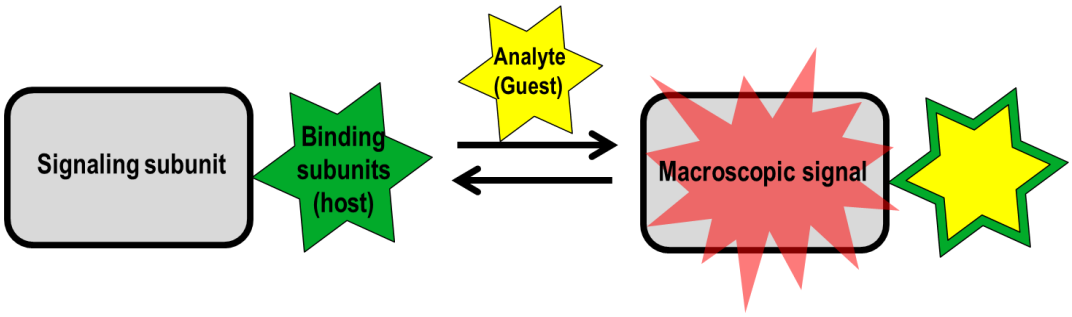

Figure 1. Schematic representation of a chemosensor based on the binding site-signaling

approach

1.1 Colorimetric sensors

Colorimetric sensors are based on changes in a material's absorption statuses, both in the absorbance intensity at a fixed wavelength and in wavelength shifts measurable by UV-Vis spectroscopy. A generally research plan is the design and synthesis of sensing probe capable of giving rise to a "naked-eye" color change upon interaction with target molecule. Therefore, colorimetric sensors are sensing methods that non-specialists can detect target compounds.

1.2 Fluorescence sensors

Fluorescence sensors are based upon changes in lifetime, intensity and wavelength, etc. These methods are broadly used and are quickly growing in chemical sensing due to the inherent sensitivity of the fluorescence technique and due to its widespread availability.

1.3 Small molecule *vs*. Polymer chemosensors

The special recognition performance of naturally happening biological processes are not based on a single molecules but in human body wherein the receptor is served by the analyte(target) removal and delivery mechanism, and the selectivity is originated from receptors as a result of analyte triggered biochemical processes.

Small molecule chemosensors mainly rely on the direct interaction of the receptor with the analyte. They can be generally divided into two main types on the basis of detection

principles, such as molecular recognition-based and chemical reaction-based small molecule sensors. Small molecule chemosensors have been often used due to their high sensitivity, selectivity and easy process. However, small molecule chemosensors usually know from some limitations such as low water solubility, low structural stability and low functionality. For overcome to these limitations, has been utilized as a novel approach such as polymer chemosensors.

Polymer chemosensors are extremely high molecular weight molecules, constituted by repeating units, and offer plenty of opportunities to couple analyte receptor interactions with intra- or intermolecular polymer interactions and solvent-polymer interactions: (a) in solution (b) in the solid state and, (c) in the highly interesting swelled and gel states. In addition to the affordable, distinct polymer geometries, that is, linear, spherical, and tridimensional (cross-linked network), the polymer constitution may be easily designed to create hydrophobic or hydrophilic environments for the pendant or main chain receptor motifs in a hydrophilic or hydrophobic medium, respectively, due to intra- and intermolecular polymer interactions and polymer-solvent interactions.

Chapter 2

Thiosemicarbazone Based Water-Soluble Polymeric Probe for the Selective Sensing and Separation of Cu(II) Ions in Aqueous Media

2.1 Abstract

A thiosemicarbazone-based water-soluble polymeric probe was developed for the selective colorimetric detection of Cu(II) ions with pH-tunable sensitivity. The successful separation of Cu(II) ions from several alkali and transition metal cations by thermal precipitation was demonstrated. N,N-Dimethylacrylamide (DMA) and 3-vinylbenzaldehyde (VBA) were copolymerized by reversible addition−fragmentation chain transfer (RAFT) polymerization to produce p(DMA-co-VBA), herein P1. The aldehyde group of P1 was reacted with 4-phenylthiosemicarbazide to yield poly, [p(DMA-co-PVHC)], herein P2. Upon the addition of Cu(II) ions to an aqueous solution of P2, the color of the solution turned from colorless to yellow due to the formation of a coordination complex between the Cu(II) ions and phenylthiosemicarbazone units of P2, herein P2−Cu(II). The availability of the electron-rich imino nitrogen in the thiosemicarbazone units allowed P2 to show excellent sensing behavior toward Cu(II) ions. P2 has remarkable pHswitchable sensing properties toward Cu(II) ions. Although efficient colorimetric sensing was observed at neutral or high pH, no appreciable color change appeared at low pH. Protonation of the imino nitrogen at low pH prevented the formation of coordination complexes. Cu(II) ions were separated successfully from various alkali and transition metal cations by thermal precipitation due to the thermoresponsive property of P2−Cu(II).We

report the unique thermoresponsive properties of fluorinated polyacrylamides, poly[N-(2,2-difluoroethyl)acrylamide] (P2F). The solubility of fluorinated polyacrylamides in water can be easily controlled by changing the number of fluorine atoms in N-ethyl groups.Moreover, we demonstrate that fluorinated polyacrylamides are less cytotoxic than poly(N-isopropylacrylamide) (PNIPAM).

Keywords.

Cu(II) ions, Polymeric sensor, Colorimetric sensor, Thiosemicarbazone, pH-tunable

2.2 Introduction

The selective detection and efficient separation of transition metal ions has become increasingly important in recent times because of their vital role in biological processes and highly toxic nature.[1-7] Among them, Cu(II) ions, being the third most abundant elements in the human body, have attracted considerable attention because they can have both positive and negative impacts on human health and the environment. Cu(II) ions are crucial components in biological processes, such as bone formation, cellular respiration, and connective tissue development and they also serve as a catalytic co-factor for several metalloenzymes.[8, 9] On the other hand, beyond a certain limit, unbound Cu(II) ions can harm the human body and environment because of their high toxicity.[10, 11] Therefore, the development of molecular probes for the rapid, selective, and efficient detection and separation of Cu(II) ions is essential in the field of chemo and biosensors.

Several methods have been used to detect Cu(II) ions, including atomic absorption spectroscopy (AAS), inductively coupled plasma-atomic emission/mass spectrometry (ICP-AES/ICP-MS), electrochemical methods, surface plasma resonance detection, and quantum dot-based assays.[12-14] Among them, colorimetric and fluorometric sensors have become increasingly popular because of their high sensitivity, qualitative and quantitative operational simplicity, and facile reactivity.[15-17]

Unlike thioureas, thiosemicarbazone moieties, which contain an additional imine group adjacent to the thiourea, provide a suitable coordination site for Cu(II) ions. Thiosemicarbazones have attracted considerable attention because of their wide range of biological properties, such as antiviral effects and antitumor activities.[18-21] Complexation with metal ions, particularly with Cu(II) ions, increases the biological activity or weakens the side effects. Although a range of optical probes, including rhodamine or fluorescein dyes and other organic chromophores, have been developed for the selective detection of Cu(II) ions, there are only a few examples of thiosemicarbazone-based sensors,[17, 22-24] which are excellent candidates for applications in optical and fluorescence cellular imaging and chemotherapeutics.

A variety of molecular probes have been reported for the detection of Cu(II) ions, but the development of chemosensors that can be used in aqueous media is still challenging.[9, 25-27] In this regard, stimuli-responsive water-soluble polymers with molecular receptor moieties or sensing units for Cu(II) ions are attractive. Compared to other conventional detection systems based on small molecular probes, stimuli-responsive polymeric probes offer enhanced water solubility, multifunctional sensing capability, and tunable detection sensitivity driven by external stimuli, such as pH, temperature, and light.[28-31]

The responsive properties of polymers have been applied to the separation of heavy metal

ions.[32] Stimuli-responsive polymers, having ligands capable of forming efficient coordination with specific heavy metal ions,[33] are expected to serve as separators and efficient chemosensors. For example, Takeshita *et al*. reported the separation of Am(III) and Eu(III) ions using a thermoresponsive poly(N-isopropylacrylamide) (PNIPAm) gel crosslinked with ligands that can form complexes specifically with those ions.[34] Tokuyama *et al*. proposed the temperature-driven solid-phase separation of Cu(II) ions using a thermoresponsive hydrogel.[35, 36]

This paper reports a polymeric probe containing thiosemicarbazone moieties for the detection and separation of Cu(II) ions in an aqueous medium. On-off Cu(II) ion detection was controlled by changing the pH of the aqueous solutions. The thermal precipitation-induced separation of Cu(II) ions among several alkali and transition metal cations was also demonstrated.

2.3 Experimental

2.3.1 Material

2,2′-Azobisisobutyronitrile (AIBN, Aldrich, 98%) was recrystallized from ethanol. 2-(dodecylthiocarbonothioylthio)-2-methylpropionic acid (DMP, 98%), 3-vinylbenzaldehyde (VBA, 97%), *N*,*N*-dimethylformamide (DMF, 99.8%), tetrahydrofuran (99.9%), 1,3,5-trioxane (99%), and N-(2-hydroxyethyl)piperazine-N'-(2-ethanesulfonic acid) (HEPES) were purchased from Aldrich. *N*,*N*-dimethylacrylamide (DMA, 99.0%) and 4-phenylthiosemicarbazide (98.0%) were obtained from TCI (Tokyo Chemical Industry) and used as received. All metal perchlorate salts were supplied by Aldrich at the highest available purity and used as received.

2.3.2 Instrumentation

^{1}H nuclear magnetic resonance (NMR, Bruker Avance 300 MHz NMR) spectroscopy was performed in DMSO-d_6. The apparent molecular weights and molecular weight distributions were measured by gel permeation chromatography (GPC, Agilent technologies 1200 series) using a polystyrene standard with DMF as the eluent at 30 ^{o}C and a flow rate of 1.00 mL/min. The UV-Vis spectra were recorded using an SINCO Mega Array PDA UV-Vis spectrophotometer equipped with a digital temperature controller. The hydrodynamic diameters were measured by dynamic light scattering (DLS, Nano ZS,

Malvern, U.K.). Inductively coupled plasma optical emission spectroscopy (ICP-OES) was carried out in an iCAP 6000 Duo (Thermo Fisher Scientific Inc., Waltham, MA, USA). Calibration was achieved using certified standard solutions from Merck (Inorganic Ventures' Quality Control Standard 26). The standard solutions were prepared at 1, 5, and 10 mg/L of a HNO_3/HF solution.

2.3.3 Synthesis

Poly[(N,N-Dimethylacrylamide)-*co*-(3-Vinylbenzaldehyde)] p(DMA-*co*-VBA) P1 N,N-Dimethylacrylamide (5 mL, 48.52 mmol), 3-vinylbenzaldehyde (0.257 mL, 2.02 mmol), DMP (184.3 g, 0.505 mmol), AIBN (4.15 mg, 0.0253 mmol), 1,3,5-trioxane (0.0455 g, 0.505 mmol, internal standard), and DMF (5 mL) were sealed in a 25 mL Schlenk flask equipped with a magnetic stirring bar at 70 ^{o}C under an argon atmosphere. The solution was purged with argon for 20 min, and the reaction flask was placed in a preheated oil bath at 70 ℃. The samples were removed periodically using a syringe to determine the molecular weight and polydispersity index (PDI) by GPC and monomer conversions by ^{1}H NMR spectroscopy. Polymerization was quenched 4 h later by exposing the mixture to air. The product was then precipitated in diethyl ether, filtered, and dried in a vacuum oven at 30 ^{o}C. M_n= 4 200 g/mol, M_w/M_n= 1.08. ^{1}H NMR (300 MHz, $CDCl_3$, δ in ppm): 9.95 (1H, s, -C*H*O); 7.75 - 7.55 (2H, s, Ar*H*); 7.55 - 7.28 (2H, s, Ar*H*); 2.85 (6H, s, -N(CH_3)$_2$)

Poly P(DMA-*co*-PVHC) P2 p(DMA-*co*-VBA) (P1, 0.69 g, 1.759 mmol per VBA repeating unit), and 4-phenylthiosemicarbazide (0.294 g, 1.759 mmol) were added to a round-bottomed flask and dissolved in THF (50 mL). The reaction mixture was heated under reflux at 80 ^{o}C overnight. After evaporating the solvent, the resulting crude product was precipitated in diethyl ether and filtered. The precipitation process was repeated three times and dried in a vacuum oven at 30 ^{o}C to give P2. M_n= 5 100 g/mol, M_w/M_n= 1.18. ^{1}H NMR (300 MHz, $CDCl_3$, δ in ppm): 11.20 - 10.0 (1H, s, -N*H*); 10.0 - 9.0 (1H, s, -N*H*); 8.60 - 7.80 (1H, s, -C*H*=N-); 7.80 - 6.80 (9H, m, Ar*H*)

2.4 Results and Discussion

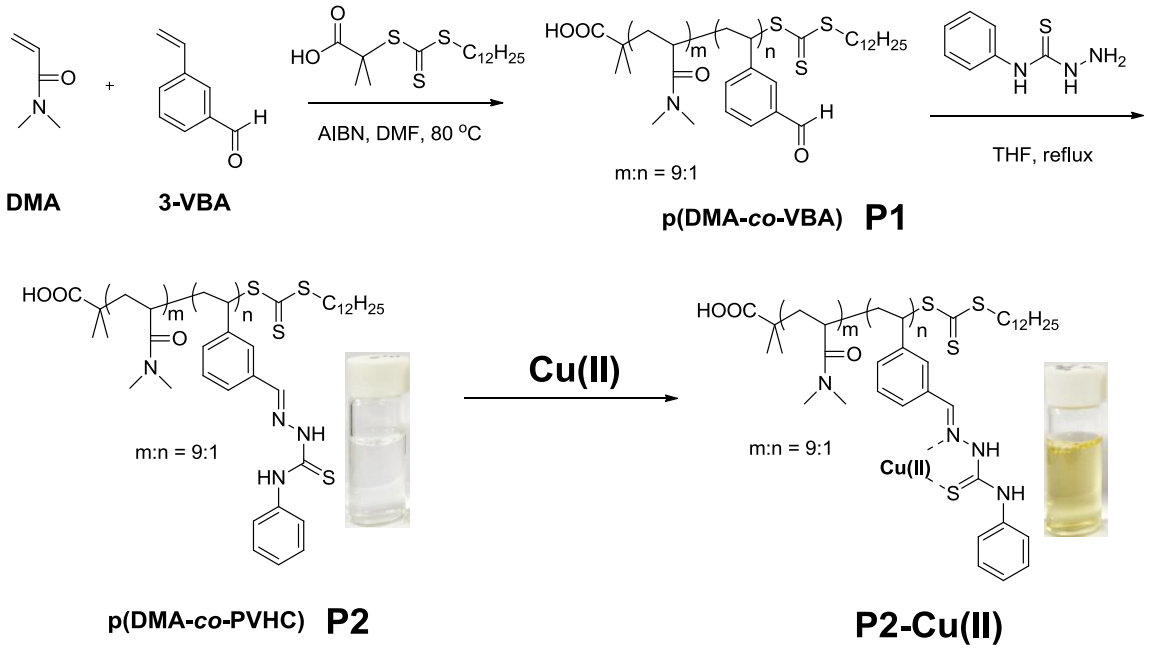

Scheme 1. RAFT random copolymerization of DMA and 3-VBA to yield p(DMA-*co*-VBA) (P1), subsequent post-modification of P1 to yield p(DMA-*co*-PVHC) (P2), and the selective detection of Cu(II) ions by the formation of coordination complexes between Cu(II) ions and phenylthiosemicarbazone units of P2 [P2-Cu(II)].

Scheme 1 presents the synthetic strategy used in this study. Reversible addition-fragmentation chain transfer (RAFT) copolymerization was used to directly prepare a p(DMA-*co*-VBA) (P1) with a well-controlled molecular weight and narrow molecular weight distribution (Figure S1). DMP was used as a chain transfer agent (CTA) and AIBN as an initiator with [DMA + 3-VBA] : [DMP] : [AIBN] = 100 : 1 : 0.05. The monomer feed ratio of DMA and 3-VBA was 96 : 4. Polymerization was quenched when the monomer conversion of DMA and 3-VBA reached 33 and 85 % in 4 h, respectively. Figure 1a presents the ^{1}H NMR spectrum of P1. The incorporation ratio of 3-VBA with respect to DMA was calculated by comparing the relative peak intensities corresponding to aldehyde protons (a) and dimethyl protons of DMA in the ^{1}H NMR spectrum of P1. The DMA : 3-VBA incorporation ratio was calculated to be 9 : 1. The final incorporation ratio of 3-VBA was higher than the initial feed ratio, suggesting that the reactivity of the styrenic monomer is higher than that of the acrylamide-based monomers. P1 was soluble in water despite approximately 10 % of hydrophobic VBA units being incorporated along the polymer chains. The number-averaged molecular weight (M_n) of P1 was 4,200 with a low molecular weight distribution (M_w / M_n = 1.08) (Figure S1).

In the next step, the aldehyde groups of P1 were reacted with 4-phenylthiosemicarbazide to yield p(DMA-*co*-PVHC) (P2). The GPC traces in Figure S1 showed a slight increase in

molecular weight after post-modification. Direct evidence of the successful transformation of P1 to P2 was confirmed by ^{1}H NMR spectroscopy (Figure 1b). The aldehyde proton of P1 originating from the 3-VBA units at 10.0 ppm disappeared completely while new peaks (j, k, and l) of P2 appeared at approximately 7.8 ~ 11.1 ppm.

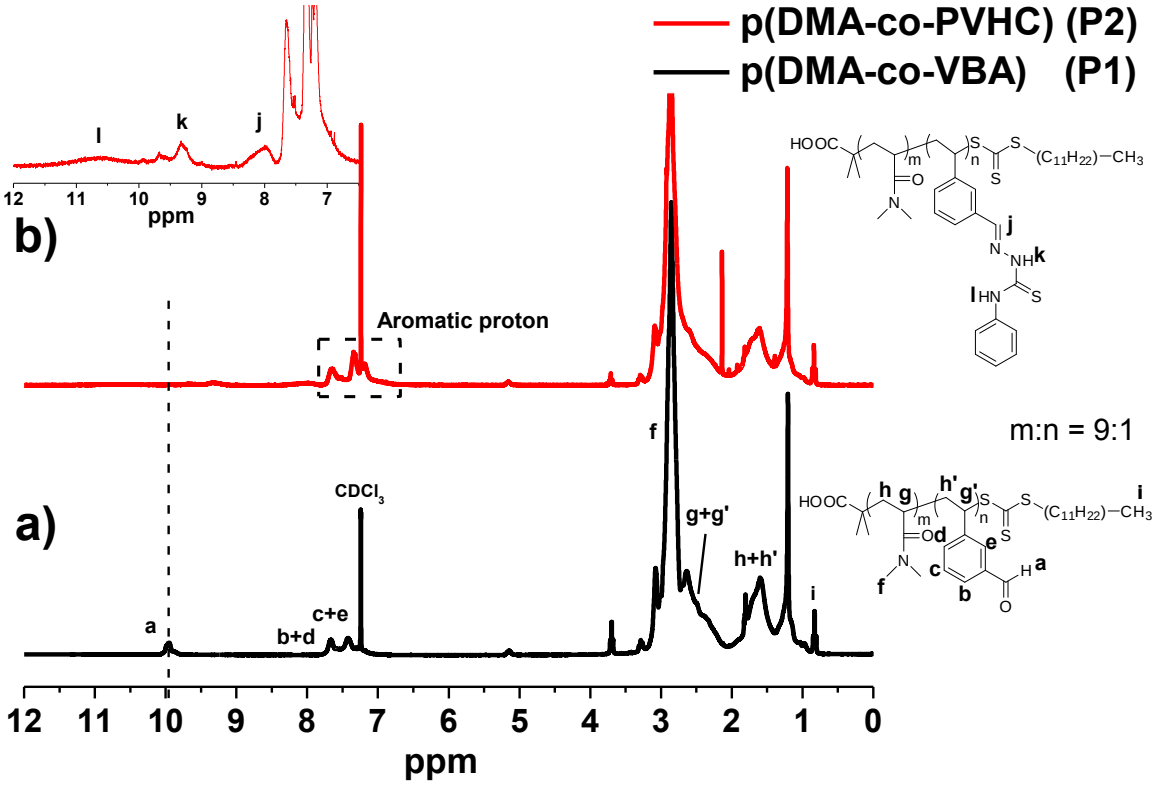

Figure 1. ^{1}H NMR spectra of a) P1 and b) P2.

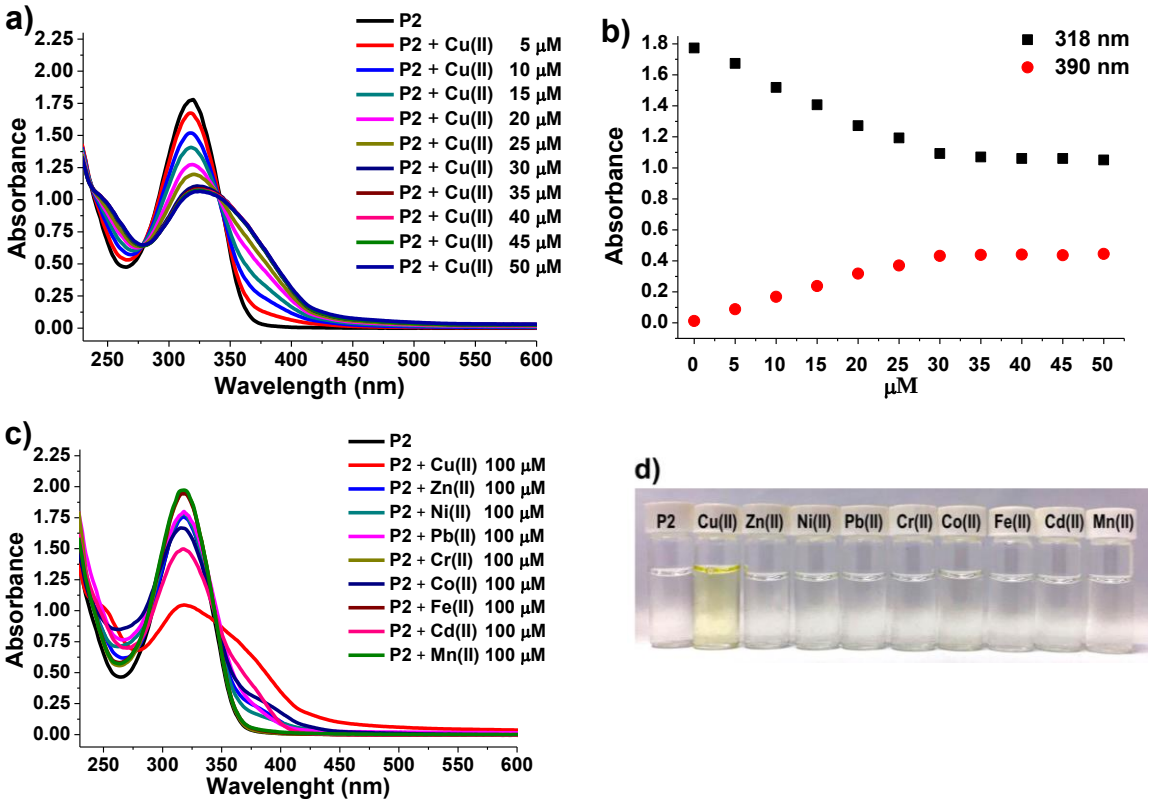

Figure 2. a) UV-Vis spectra of P2 (50 µM of the phenylthiosemicarbazone units along the P2 chain) upon the gradual addition of an aqueous solution of Cu(II) ions. b) Absorbance at 318 nm and 390 nm versus the amount of Cu(II) added. c) UV-Vis spectra and d) photographs of P2 (50 µM of phenylthiosemicarbazone units) upon the addition of various metal cations (100 µM) in HEPES buffer.

The Cu(II) ion sensing studies with P2 were carried out in HEPES buffer at pH 7.4. The aqueous solution of P2 (3.0 mL, 0.01 wt%) was prepared in a 50 μM concentration of phenylthiosemicarbazone moieties (assuming 10 % incorporation of phenylthiosemicarbazone moieties along the polymer chain). The solution of Cu(II) ions (3.0 mM) was prepared in HEPES buffer solution. The UV-Vis absorption spectral changes in P2 with the gradual addition of Cu(II) ions in the concentration range of 5-50 μM (5-50 μM) were monitored (Figure 2a). The UV-Vis absorption spectrum of the original P2 solution showed a maximum at 318 nm. Upon the gradual addition of Cu(II) ions, the absorption maximum at 318 nm was decreased progressively and red-shifted to 328 nm with an isosbestic point at 350 nm while the overall absorption bands broadened. Figure 2b shows plots of the Cu(II) concentration versus absorbance at 318 and 390 nm. The reason why the wavelength of 390 nm was plotted is that wavelengths shorter than 390 nm are part of the UV spectrum and are not visible, and 390 nm is the onset of the greenish yellow color.[37-39] The decrease at 318 nm and the increase in absorbance at 390 nm were monitored upon the gradual addition of Cu(II) ions up to 35 μM, above which no further change was observed. Consequently, the color of the P2 solution turned from colorless to greenish yellow, which could be seen easily by the naked eye. The reason for the change in solution color was attributed to the formation of coordination complexes between Cu(II)

ions and phenylthiosemicarbazone units of P2 [P2-Cu(II)]. The detection limit of P2 toward Cu(II) ions was as low as 5.0 μM. In addition to their high sensitivity, P2 exhibited good selectivity toward Cu(II) ions over several alkali and transition metal cations [Zn(II), Ni(II), Pb(II), Cr(II), Co(II), Fe(II), Cd(II), and Mn(II)] (Figure 2c and S2). Small changes in UV-Vis spectra were observed for the other cations but the colorimetric changes were not significant. Pyridine-based thiosemicarbazones usually bind with Zn(II) or Fe(II) through tridendate coordination. In this work, phenylthiosemicarbazone facilitated bidendate coordination selectively with Cu(II).[40-42] This unique sensing behavior can be observed directly in the photograph (Figure 2d).

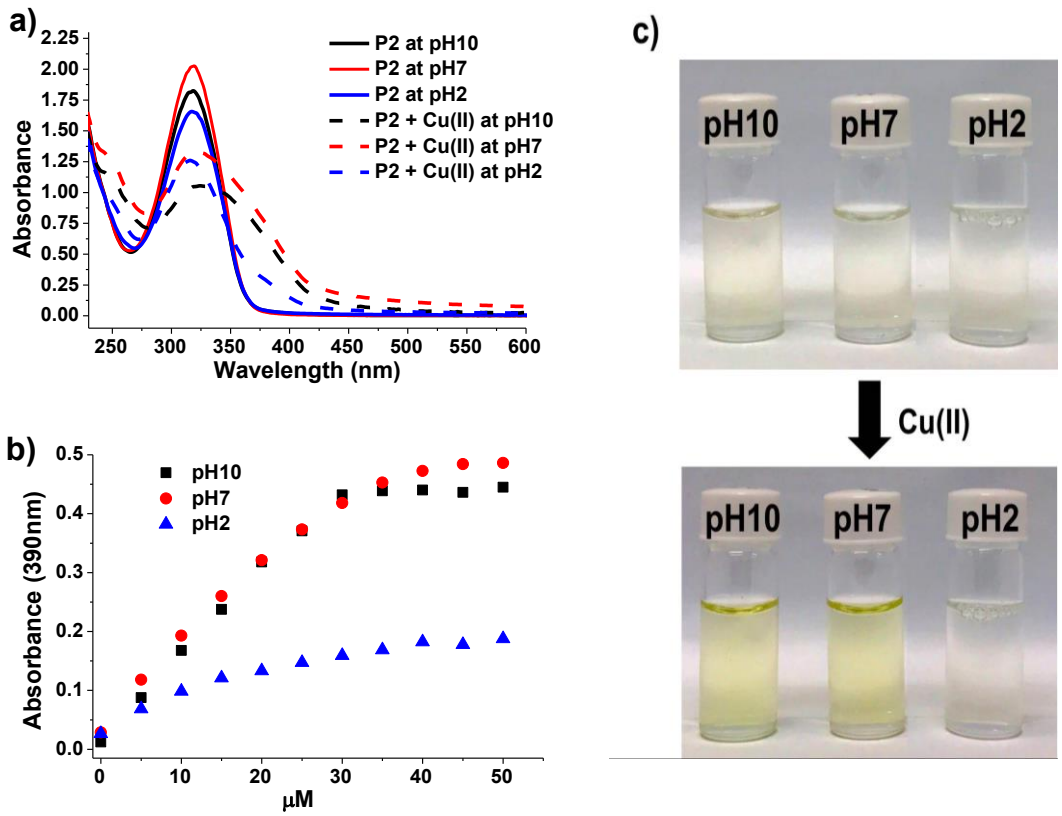

Figure 3. a) UV-Vis spectra and b) photographs of P2 (50 μM of phenylthiosemicarbazone units along the P2 chain) upon the addition of Cu(II) ions (50 μM) at different pH values. c) Changes in absorbance at 390 nm upon the gradual addition of Cu(II) ions at different pH.

After demonstration of the selective and sensitive detection of Cu(II) ions with P2, pH-dependent control of the detection of Cu(II) ions was attempted. For this, the UV-Vis spectra of the P2 solution were examined at different pH after the addition of 50 μM Cu(II) ions (Figure 3a). As expected, the $\Delta\lambda_{max}$ of the solution at pH 7 showed a 10 nm red-shift with spectral broadening after the addition of Cu(II) ions. This suggests that the formation of P2-Cu(II) coordination complexes can be achieved easily at high pH. Note that similar phenomena were observed for the P2 solution at pH 10. Interestingly, there was no shift in the absorption maximum after the addition of Cu(II) ions at pH 2 but there was some spectral broadening (Figure 3a). These results were clearly reflected in the photograph in Figure 3b. No color change was observed for the aqueous solution of P2 at pH 2 upon the addition of Cu(II) ions, but there were discernable color changes at pH 7 and 10. Figure 3c presents plots of the Cu(II) concentration versus absorbance at 390 nm at different pH. While there was a slight increase in absorbance at 390 nm at pH 2, a notable increase at pH 7 and 10 was observed. The formation of P2-Cu(II) coordination complexes was hindered somewhat at low pH. The sensitivity of P2 on Cu(II) ions decreased with decreasing pH of the solution. This suggests that the pH-dependent sensitivity is related directly to the effective formation of P2-Cu(II) coordination complexes.

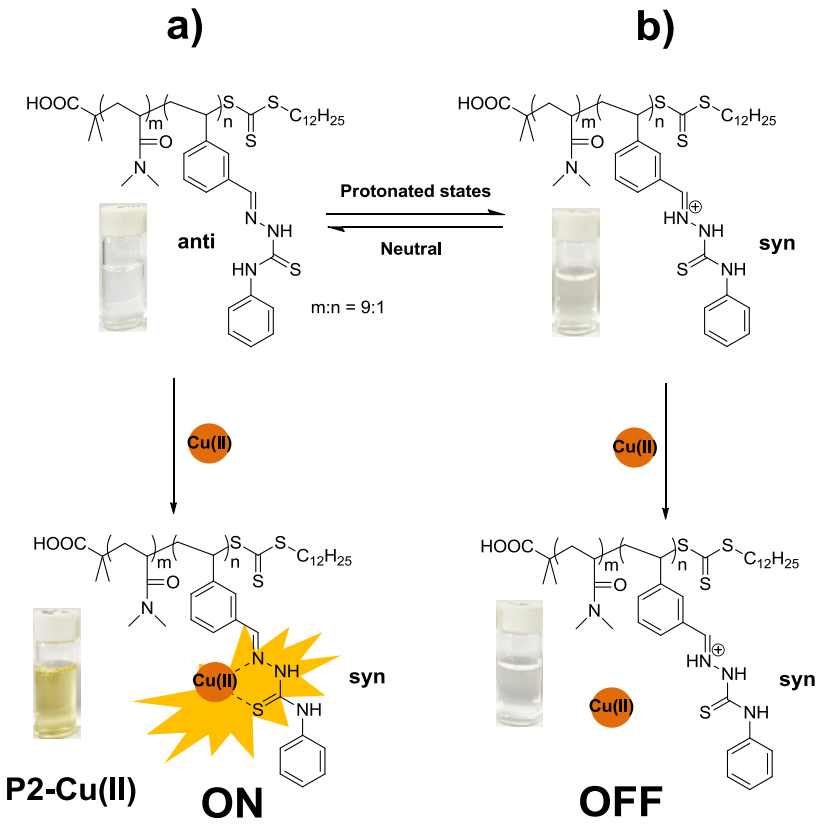

Figure 4. Schematic diagram of the colorimetric detection of Cu(II) ions with tunable detection sensitivity driven by a change in pH in the aqueous solution; a) high pH (tertiary amine with lone pair electrons): the formation of P2-Cu(II) coordination complexes via thiourea sulfur and imino nitrogen atoms through a rearrangement of the thiourea moiety to a favorable syn-conformation, and b) low pH (quaternary amine salt): no formation of P2-Cu(II) coordination complexes due to the protonation of imino nitrogen atoms.

The proton exchange reaction between the neutral and protonated states was observed on the phenylthiosemicarbazone moieties. In the neutral state, thiourea is favored to have a intramolecular hydrogen bonding-assisted anti-conformation.[19, 29] Upon the addition of Cu(II) ions, complexation with Cu(II) ions via thiourea sulfur and imino nitrogen atoms can be achieved through conformational changes of thiourea to a syn conformation, enabling the active detection of Cu(II) ions. In the protonated state (low pH), a conformational change from anti to syn occurs upon the protonation of imino nitrogen atom of phenylthiosemicarbazone moieties. Protonation of the imino nitrogen led to quaternary cations. In other words, the lone pair electrons necessary for the complexation with Cu(II) ions were unavailable. As a result, the formation of P2-Cu(II) coordination complexes was prevented, leading to an OFF-state for the detection of Cu(II) ions.

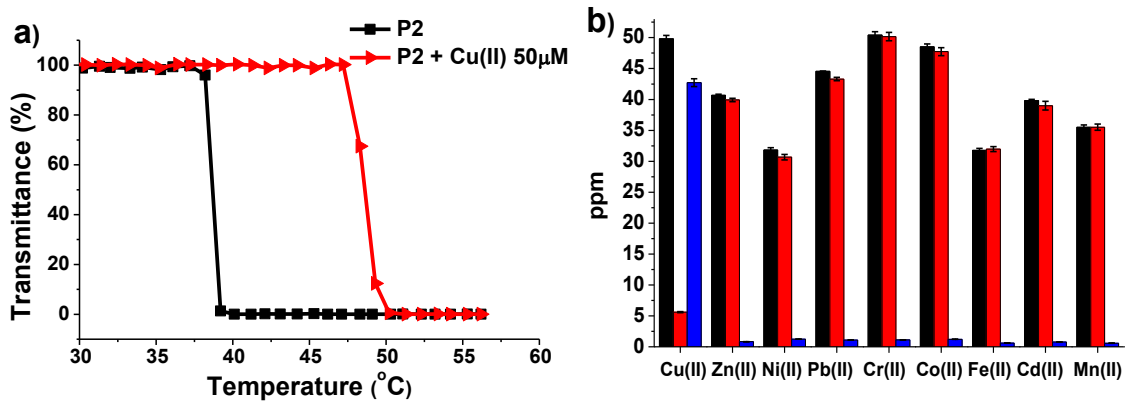

Figure 5. a) Plots of the transmittance as a function of temperature measured on P2 (10 mg/mL) and P2-Cu(II) coordination complexes (after the addition of 50 μM of Cu(II) ions) by turbidimetry and b) ICP-OES measurements; black column: the concentration of the original aqueous solution containing various metal cations (50 ppm of each metal cations was targeted initially), red column: concentration of various metal cations from the remaining solution after the addition of P2 (1.0 wt%), followed by the separation of Cu(II) ions by thermal precipitation, blue column: concentration of various metal cations from the separated polymer

The thermal phase transition is influenced by the monomer composition of copolymers that governs the hydrophilicity/hydrophobicity balance.[43-45] PDMA is hydrophilic. Therefore, it does not have a lower critical solution temperature (LCST) up to 100 ^{o}C. The small incorporation of hydrophobic PVHC units along the polymer chains allows P2 to exhibit an LCST. The thermal transition in solubility was examined by observing the changes in the percentage transmission at a fixed wavelength (650 nm) by UV-Vis spectroscopy. The LCST point of the aqueous solutions (1.0 wt%) of P2 was detected at 38 ^{o}C (Figure 5a). After adding 50 μM of Cu(II) ions to this P2 solution, the LCST of P2-Cu(II) coordination complexes was increased further to 47 ^{o}C. The formation of complex ions by coordinate interactions would render the polymers more hydrophilic, leading to an increase in the LCST value (Figure 5a). The effects of the formation of P2-Cu(II) coordination complexes on the LCST point were also examined by dynamic light scattering (DLS) at the same aqueous concentration (10 mg/mL) as that used for turbidimetry studies. The DLS data were recorded during the heating cycles. The LCST point was defined as the onset temperature of the increase in particle size. These LCST values determined by DLS were matched well with those determined by turbidimetry (Figure S3).

Having shown the thermal phase transition behaviors of the P2-Cu(II) coordination complexes, the efficient separation of Cu(II) ions among other metal cations was attempted.

This separation was made possible by the thermoresponsive nature of the P2-Cu(II) coordination complexes; upon heating the P2-Cu(II) coordination complexes above the LCST (47 ^{o}C), only P2-Cu(II) precipitated from an aqueous solution, leaving other metal cations intact, thereby facilitating the separation of Cu(II) ions from other metal cations. ICP-OES was used to evaluate the efficacy of the separation of Cu(II) ions by thermal precipitation. An aqueous solution of various metal cations (each with 50 ppm, 0.5 mg of each metal cation/10 mL of deionized water) was prepared. To this solution, 0.1 g of P2 (0.5 mM of phenylthiosemicarbazone units) was added. The resulting solution was then stirred and heated at 55 ^{o}C for 30 sec, resulting in precipitates stuck to the vial. The remaining solution was separated from the precipitates and subjected to ICP-OES. The precipitates containing Cu(II) ions [P2-Cu(II)] were redissolved in 10 mL of cold deionized water and examined by ICP-OES. Figure 5b shows the results of ICP-OES (see also Figure S4 for raw data). Before adding P2, the quantity of metal ions of the original solution ranged from 30 to 50 ppm (black column). After adding P2, followed by thermal precipitation, only 5 ppm of Cu(II) ions (90 % removal) were detected from the remaining solution with no noticeable reduction in the concentration of other metal ions observed (red column). This efficient separation of Cu(II) ions by thermal precipitation was further demonstrated by analyzing the precipitates. The precipitates contained more than 40 ppm

Cu(II) ions (more than 80 % recovery) while no significant quantity of other metal ions were detected (blue column).

2.5 Conclusions

Well-defined water-soluble p(DMA-*co*-PVHC) copolymer for the efficient detection of Cu(II) ions was synthesized by RAFT polymerization, followed by post-modification reactions. The selective colorimetric sensing of Cu(II) ions in aqueous media described here rely on the formation of coordination complexes between Cu(II) ions and the phenylthiosemicarbazone units of the polymeric probes. The formation of these complexes was tuned finely by the variation in pH of the aqueous solution, which in turn governed the detection switchability: active colorimetric sensing at neutral or high pH, but no sensing at low pH due to the less facile formation of coordination complexes by protonation on the imino nitrogen of the phenylthiosemicarbazone units. Furthermore, the superior separation of Cu(II) ions from the other metal cations by thermal precipitation was explained by the thermoresponsive property of these complexes. The pH-switchable detection of Cu(II) ions coupled with temperature-induced separation is expected to have many applications in tunable sensing and separation.

2.6 Supplementary Information

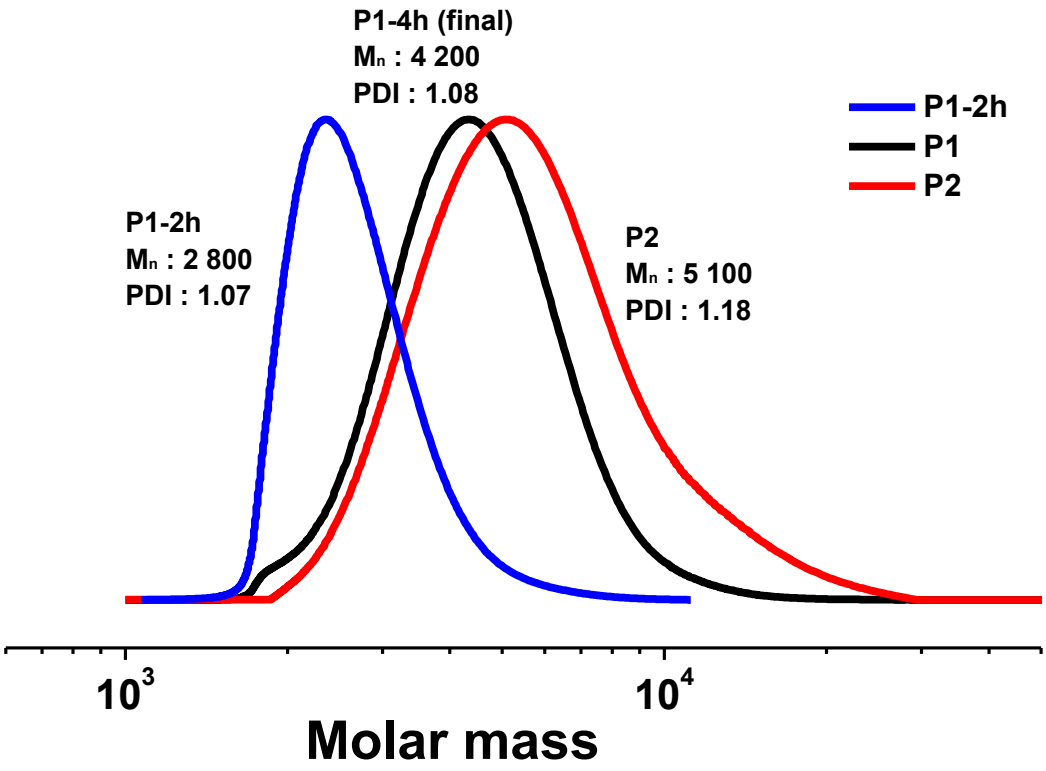

Figure S1. DMF GPC traces of P1 and P2 copolymer.

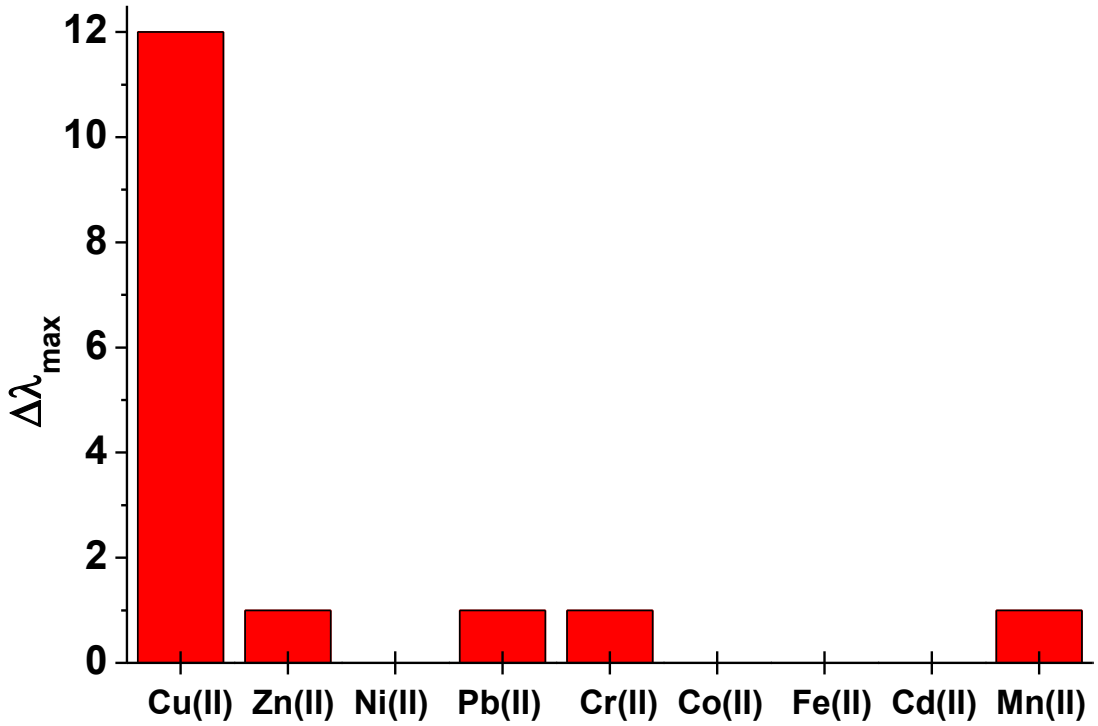

Figure S2. The selectivity bar diagram of P2 copolymer with various cations in aqueous solution at 25 ^{o}C. The absorption maximum $\Delta\lambda_{max}$ ($\Delta\lambda_{max} = \lambda_0-\lambda_\chi$, λ_0 is the absorption maximum with P2 (50 μM) and λ_χ is absorption maximum with various cations (6.0 x 10^{-2} M, added to 5μL).

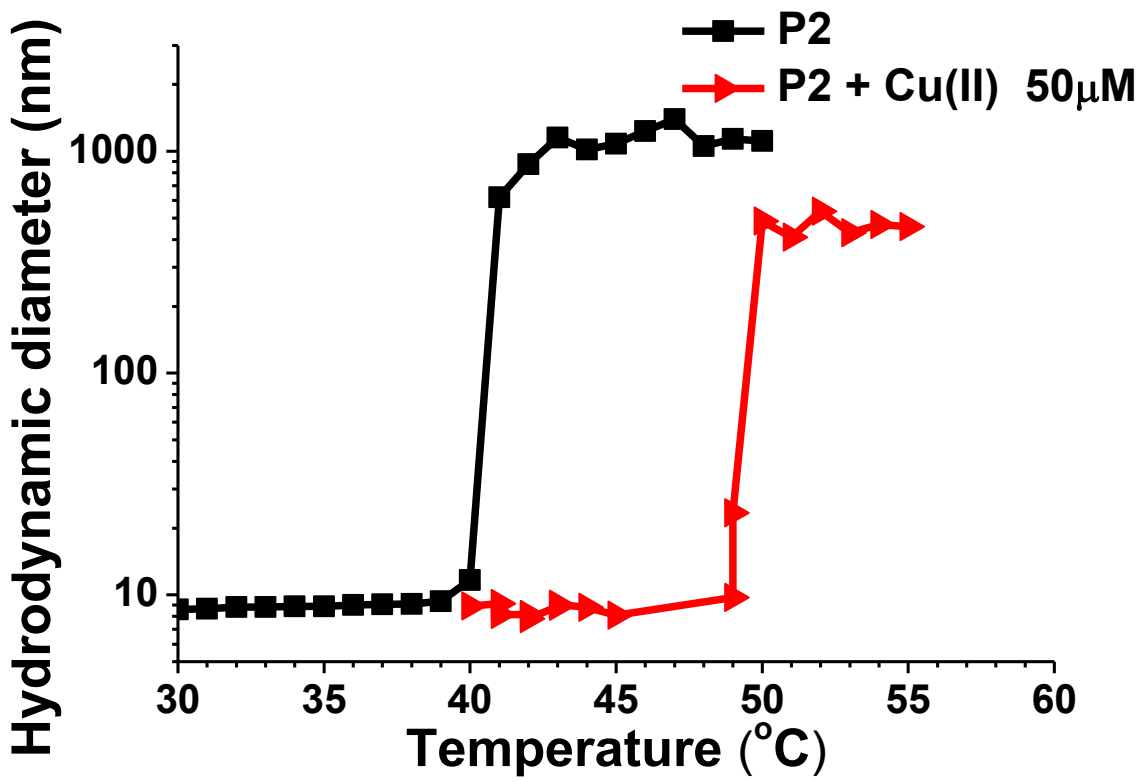

Figure S3. Plots of apparent hydrodynamic diameters as a function of temperature measured by DLS for the aqueous solution (10 mg/mL) of the original P2 and P2 + Cu(II) ion complexes (after the addition of 50 μM of Cu(II) ions)

1	Unk: sample1	2017-09-12 16:21:21	CONC							
Black column	Custom ID1:	Custom ID2:	Custom ID3:							
	Cd2288	Co2286	Cr2835	Cu3247	Fe2599	Mn2576	Ni2216	Pb2203	Sn1899	Zn2138
Units	ppm	ppm	ppm	ppm	ppm	ppm	ppm	ppm	ppm	ppm
Avg	**39.81**	**48.51**	**50.41**	**49.81**	**31.76**	**35.50**	**31.82**	**44.56**	**93.56**	**40.68**
Stddev	.20	.46	.56	.55	.32	.38	.39	.03	52.52	.16
% RSD	.5104	.9492	1.110	1.107	1.015	1.082	1.231	.0565	56.13	.3909
Rep #1	39.98	48.09	50.41	49.76	31.81	35.45	31.45	44.54	113.4	40.50
Rep #2	39.86	48.44	50.98	50.38	32.06	35.90	31.77	44.58	133.3	40.75
Rep #3	39.58	49.01	49.86	49.28	31.42	35.14	32.23	44.55	34.01	40.79
2	Unk: sample2	2017-09-12 16:24:49	CONC							
Red column	Custom ID1:	Custom ID2:	Custom ID3:							
	Cd2288	Co2286	Cr2835	Cu3247	Fe2599	Mn2576	Ni2216	Pb2203	Sn1899	Zn2138
Units	ppm	ppm	ppm	ppm	ppm	ppm	ppm	ppm	ppm	ppm
Avg	**38.99**	**47.73**	**50.17**	**5.610**	**31.98**	**35.52**	**30.67**	**43.30**	**-274.4**	**39.92**
Stddev	.70	.64	.67	.082	.40	.49	.45	.28	61.8	.27
% RSD	1.802	1.347	1.341	1.455	1.243	1.393	1.462	.6558	22.51	.6682
Rep #1	39.74	48.47	50.51	5.644	32.18	35.75	31.01	43.59	-318.6	40.21
Rep #2	38.35	47.31	49.40	5.517	31.52	34.95	30.16	43.03	-203.8	39.69
Rep #3	38.87	47.41	50.61	5.670	32.23	35.86	30.84	43.28	-300.8	39.85
3	Unk: sample3	2017-09-12 16:28:00	CONC							
Blue column	Custom ID1:	Custom ID2:	Custom ID3:							
	Cd2288	Co2286	Cr2835	Cu3247	Fe2599	Mn2576	Ni2216	Pb2203	Sn1899	Zn2138
Units	ppm	ppm	ppm	ppm	ppm	ppm	ppm	ppm	ppm	ppm
Avg	**.7769**	**1.216**	**1.111**	**42.71**	**.6052**	**.5857**	**1.237**	**1.095**	**-932.9**	**.8203**
Stddev	.0082	.012	.019	.64	.0129	.0073	.011	.007	46.0	.0083
% RSD	1.056	.9876	1.735	1.503	2.136	1.246	.9013	.6230	4.930	1.008
Rep #1	.7701	1.205	1.111	42.55	.5938	.5843	1.228	1.089	-980.7	.8136
Rep #2	.7745	1.213	1.091	42.17	.6027	.5791	1.233	1.093	-929.1	.8178
Rep #3	.7860	1.229	1.130	43.42	.6193	.5935	1.249	1.102	-889.0	.8296

Figure S4. Raw data of ICP-OES measurements.

2.7 References

1. Balamurugan, A.; Lee, H.-i. Aldoxime-Derived Water-Soluble Polymer for the Multiple Analyte Sensing: Consecutive and Selective Detection of Hg2+, Ag+, ClO–, and Cysteine in Aqueous Media. *Macromolecules* **2015,** 48 (12), 3934-3940 DOI: 10.1021/acs.macromol.5b00731.
2. Gupta, M.; Balamurugan, A.; Lee, H.-i. Azoaniline-based rapid and selective dual sensor for copper and fluoride ions with two distinct output modes of detection. *Sens. Actuator B-Chem.* **2015,** 211, 531-536 DOI: 10.1016/j.snb.2015.01.125.
3. Balamurugan, A.; Lee, H.-i. Water-Soluble Polymeric Probes for the Selective Sensing of Mercury Ion: pH-Driven Controllable Detection Sensitivity and Time. *Macromolecules* **2015,** 48 (4), 1048-1054 DOI: 10.1021/ma502350p.
4. Gupta, M.; Lee, P. H.-i. A dual responsive molecular probe for the efficient and selective detection of nerve agent mimics and copper (II) ions with controllable detection time. *Sens. Actuator B-Chem.* **2017,** 242, 977-982 DOI: 10.1016/j.snb.2016.09.156.
5. Chie, K.; Fujiwara, M.; Fujiwara, Y.; Tanimoto, Y. Magnetic separation of metal ions. *J. Phys. Chem. B* **2003,** 107 (51), 14374-14377.
6. Czarnik, A. W. Chemical communication in water using fluorescent chemosensors. *Acc. Chem. Res.* **1994,** 27 (10), 302-308.
7. De Silva, A. P.; Gunaratne, H. N.; Gunnlaugsson, T.; Huxley, A. J.; McCoy, C. P.; Rademacher, J. T.; Rice, T. E. Signaling recognition events with fluorescent sensors and switches. *Chem Rev.* **1997,** 97 (5), 1515-1566.
8. Solomons, N. W. On the assessment of zinc and copper nutriture in man. *Am. J. Clin. Nutr.* **1979**.
9. Chen, X.; Pradhan, T.; Wang, F.; Kim, J. S.; Yoon, J. Fluorescent chemosensors based on spiroring-opening of xanthenes and related derivatives. *Chem Rev.* **2011,** 112 (3), 1910-1956.
10. Multhaup, G.; Schlicksupp, A.; Hesse, L.; Beher, D.; Ruppert, T.; Masters, C. L.; Beyreuther, K. The amyloid precursor protein of Alzheimer's disease in the reduction of copper (II) to copper (I). *Science* **1996**, 1406-1409.
11. Løvstad, R. A. A kinetic study on the distribution of Cu (II)-ions between albumin and transferrin. *BioMetals* **2004,** 17 (2), 111-113.
12. Chan, M.-S.; Huang, S.-D. Direct determination of cadmium and copper in seawater using a transversely heated graphite furnace atomic absorption spectrometer with Zeeman-effect background corrector. *Talanta* **2000,** 51 (2), 373-380.

13. Butler, O. T.; Cairns, W. R.; Cook, J. M.; Davidson, C. M. Atomic spectrometry update. Environmental analysis. *J. Anal. At. Spectrom.* **2012,** 27 (2), 187-221.
14. Li, Y.; Chen, C.; Li, B.; Sun, J.; Wang, J.; Gao, Y.; Zhao, Y.; Chai, Z. Elimination efficiency of different reagents for the memory effect of mercury using ICP-MS. *J. Anal. At. Spectrom.* **2006,** 21 (1), 94-96.
15. Angupillai, S.; Hwang, J.-Y.; Lee, J.-Y.; Rao, B. A.; Son, Y.-A. Efficient rhodamine-thiosemicarbazide-based colorimetric/fluorescent 'turn-on'chemodosimeters for the detection of Hg 2+ in aqueous samples. *Sens. Actuator B-Chem.* **2015,** 214, 101-110.
16. Goswami, S.; Sen, D.; Das, N. K. A new highly selective, ratiometric and colorimetric fluorescence sensor for Cu2+ with a remarkable red shift in absorption and emission spectra based on internal charge transfer. *Org. Lett.* **2010,** 12 (4), 856-859.
17. Udhayakumari, D.; Velmathi, S.; Chen, W.-C.; Wu, S.-P. A dual-mode chemosensor: Highly selective colorimetric fluorescent probe for Cu 2+ and F− ions. *Sens. Actuator B-Chem.* **2014,** 204, 375-381.
18. Tavallali, H.; Deilamy-Rad, G.; Moaddeli, A.; Asghari, K. A new pincer-type "naked-eye" colorimetric probe for Cu 2+ determination in 80% water media and its application as a solid state sensor and an efficient antibacterial product. *Sens. Actuator B-Chem.* **2017,** 244, 1121-1128.
19. Howe, E. N.; Busschaert, N.; Wu, X.; Berry, S. N.; Ho, J.; Light, M. E.; Czech, D. D.; Klein, H. A.; Kitchen, J. A.; Gale, P. A. pH-regulated nonelectrogenic anion transport by phenylthiosemicarbazones. *J. Am. Chem. Soc.* **2016,** 138 (26), 8301-8308.
20. Richardson, D. R.; Kalinowski, D. S.; Richardson, V.; Sharpe, P. C.; Lovejoy, D. B.; Islam, M.; Bernhardt, P. V. 2-Acetylpyridine thiosemicarbazones are potent iron chelators and antiproliferative agents: redox activity, iron complexation and characterization of their antitumor activity. *J. Med. Chem.* **2009,** 52 (5), 1459-1470.
21. Afrasiabi, Z.; Sinn, E.; Padhye, S.; Dutta, S.; Padhye, S.; Newton, C.; Anson, C. E.; Powell, A. K. Transition metal complexes of phenanthrenequinone thiosemicarbazone as potential anticancer agents: synthesis, structure, spectroscopy, electrochemistry and in vitro anticancer activity against human breast cancer cell-line, T47D. *J. Inorg. Biochem.* **2003,** 95 (4), 306-314.
22. Hameed, A.; Yaqub, M.; Hussain, M.; Hameed, A.; Ashraf, M.; Asghar, H.; Naseer, M. M.; Mahmood, K.; Muddassar, M.; Tahir, M. N. Coumarin-based thiosemicarbazones as potent urease inhibitors: synthesis, solid state self-assembly and molecular docking. *RSC Adv.* **2016,** 6 (68), 63886-63894.
23. Hameed, A.; Khan, K. M.; Zehra, S. T.; Ahmed, R.; Shafiq, Z.; Bakht, S. M.; Yaqub, M.; Hussain, M.; de León, A. d. l. V.; Furtmann, N. Synthesis, biological

evaluation and molecular docking of N-phenyl thiosemicarbazones as urease inhibitors. *Bioorg. Chem.* **2015,** 61, 51-57.

24. Abid, M.; Azam, A. Synthesis and antiamoebic activities of 1-N-substituted cyclised pyrazoline analogues of thiosemicarbazones. *Bioorg. Med. Chem.* **2005,** 13 (6), 2213-2220.

25. Liu, Z.; Li, Y.; Ding, Y.; Yang, Z.; Wang, B.; Li, Y.; Li, T.; Luo, W.; Zhu, W.; Xie, J. Water-soluble and highly selective fluorescent sensor from naphthol aldehyde-tris derivate for aluminium ion detection. *Sens. Actuator B-Chem.* **2014,** 197, 200-205.

26. Guo, Z.; Zhu, W.; Tian, H. Hydrophilic copolymer bearing dicyanomethylene-4 H-pyran moiety as fluorescent film sensor for Cu2+ and pyrophosphate anion. *Macromolecules* **2009,** 43 (2), 739-744.

27. Rivas, B. L.; Pooley, S. A.; Luna, M. Chelating properties of poly (N-acryloyl piperazine) by liquid-phase polymer-based retention (LPR) technique. *Macromol. Rapid Commun.* **2000,** 21 (13), 905-908.

28. Graillot, A.; Djenadi, S.; Faur, C.; Bouyer, D.; Monge, S.; Robin, J.-J. Removal of metal ions from aqueous effluents involving new thermosensitive polymeric sorbent. *Water Sci. Technol.* **2013,** 67 (6), 1181-1187.

29. Mattiasson, B.; Kumar, A.; Ivanov, A. E.; Galaev, I. Y. Metal-chelate affinity precipitation of proteins using responsive polymers. *Nat. Protoc.* **2007,** 2 (1), 213.

30. McQuade, D. T.; Pullen, A. E.; Swager, T. M. Conjugated polymer-based chemical sensors. *Chem Rev.* **2000,** 100 (7), 2537-2574.

31. Belger, C.; Weis, J. G.; Egap, E.; Swager, T. M. Colorimetric stimuli-responsive hydrogel polymers for the detection of nerve agent surrogates. *Macromolecules* **2015,** 48 (21), 7990-7994.

32. Rao, T. P.; Daniel, S.; Gladis, J. M. Tailored materials for preconcentration or separation of metals by ion-imprinted polymers for solid-phase extraction (IIP-SPE). *TrAC, Trends Anal. Chem.* **2004,** 23 (1), 28-35.

33. Moreno-Villoslada, I.; Rivas, B. L. Competition of divalent metal ions with monovalent metal ions on the adsorption on water-soluble polymers. *J. Phys. Chem. B* **2002,** 106 (38), 9708-9711.

34. Takeshita, K.; Matsumura, T.; Nakano, Y. Separation of americium (III) and europium (III) by thermal-swing extraction using thermosensitive polymer gel. *Prog. Nucl. Energy* **2008,** 50 (2), 466-469.

35. Tokuyama, H.; Iwama, T. Temperature-swing solid-phase extraction of heavy metals on a poly (N-isopropylacrylamide) hydrogel. *Langmuir* **2007,** 23 (26), 13104-13108.

36. Tokuyama, H.; Hisaeda, J.; Nii, S.; Sakohara, S. Removal of heavy metal ions and humic acid from aqueous solutions by co-adsorption onto thermosensitive polymers. *Sep. Purif. Technol.* **2010,** 71 (1), 83-88.
37. Noh, J. Y.; Park, G. J.; Na, Y. J.; Jo, H. Y.; Lee, S. A.; Kim, C. A colorimetric "naked-eye" Cu (II) chemosensor and pH indicator in 100% aqueous solution. *Dalton Trans.* **2014,** 43 (15), 5652-5656.
38. Park, G. J.; You, G. R.; Choi, Y. W.; Kim, C. A naked-eye chemosensor for simultaneous detection of iron and copper ions and its copper complex for colorimetric/fluorescent sensing of cyanide. *Sens. Actuator B-Chem.* **2016,** 229, 257-271.
39. Elmas, Ş. N. K.; Ozen, F.; Koran, K.; Yilmaz, I.; Gorgulu, A. O.; Erdemir, S. Coumarin based highly selective "off-on-off" type novel fluorescent sensor for Cu2+ and S2− in aqueous solution. *J Fluoresc.* **2017,** 27 (2), 463-471.
40. Easmon, J.; Pürstinger, G.; Heinisch, G.; Roth, T.; Fiebig, H. H.; Holzer, W.; Jäger, W.; Jenny, M.; Hofmann, J. Synthesis, cytotoxicity, and antitumor activity of copper (II) and iron (II) complexes of 4 N-azabicyclo [3.2. 2] nonane thiosemicarbazones derived from acyl diazines. *J. Med. Chem.* **2001,** 44 (13), 2164-2171.
41. Puchta, R.; Shaban, S. Y.; Mansour, H.; Alzoubi, B. M. Structural study of 2-pyridine-derived N (4)-p-tolyl thiosemicarbazone zinc (II) complexes–DFT analysis. *J. Coord. Chem.* **2010,** 63 (14-16), 2879-2887.
42. Popović-Bijelić, A.; Kowol, C. R.; Lind, M. E.; Luo, J.; Himo, F.; Enyedy, É. A.; Arion, V. B.; Gräslund, A. Ribonucleotide reductase inhibition by metal complexes of Triapine (3-aminopyridine-2-carboxaldehyde thiosemicarbazone): A combined experimental and theoretical study. *J. Inorg. Biochem.* **2011,** 105 (11), 1422-1431.
43. Bak, J. M.; Kim, K.-B.; Lee, J.-E.; Park, Y.; Yoon, S. S.; Jeong, H. M.; Lee, H.-i. Thermoresponsive fluorinated polyacrylamides with low cytotoxicity. *Polym. Chem.* **2013,** 4 (7), 2219-2223.
44. Bak, J. M.; Lee, H. i. Novel thermoresponsive fluorinated double-hydrophilic poly {[N-(2, 2-difluoroethyl) acrylamide]-b-[N-(2-fluoroethyl) acrylamide]} block copolymers. *J. Polym. Sci. A* **2013,** 51 (9), 1976-1982.
45. Balamurugan, A.; Lee, H.-i. A water-soluble polymer for selective colorimetric sensing of cysteine and homocysteine with temperature-tunable sensitivity. *Polym. Chem.* **2014,** 5 (15), 4446-4449.

Chapter 3

Thiosemicarbazone Based Polymeric for the Sustained Release of a Model Drug via Selective Detection of Cu(II) ions

3.1 Abstract

The well-defined amphiphilic phenylthiosemicarbazone-based block copolymer was successfully synthesized by reversible addition-fragmentation chain transfer (RAFT) polymerization, followed by post-polymerization modification. Poly(*N*,*N*-dimethylacrylamide) (pDMA) was synthesized via RAFT polymerization of *N*,*N*-dimethylacrylamide (DMA). The resulting pDMA macro chain transfer agent (macroCTA) was further chain extended with 3-vinylbenzaldehyde (VBA) to yield poly[(*N*,*N*-dimethylacrylamide)-*b*-(3-vinylbenzaldehyde)] p(DMA-*b*-VBA) block copolymer. The aldehyde group of p(DMA-*b*-VBA) was reacted with 4-phenylthiosemicarbazide to yield poly{*N*,*N*-dimethylacrylamide-*b*-[*N*-phenyl-2-(3-vinylbenzylidene)hydrazine carbothioamide]}, [p(DMA-*b*-PVHC)]. p(DMA-*b*-PVHC) was self-assembled in aqueous solution to yield polymeric micelles that consist of a pDMA block forming a hydrophilic shell and pPVHC block forming a hydrophobic core. p(DMA-*b*-PVHC) micelles can detect Cu(II) ions via color changes from colorless to yellow, induced by the formation of coordination complexes between Cu(II) ions and phenylthiosemicarbazone units of p(DMA-*b*-PVHC) micelles. The core of p(DMA-*b*-PVHC) micelles was crosslinked via the slow penetration of Cu(II) ions into the core, and the resulting particles with crosslinked ionic cores became swollen in water. Upon the addition of Cu(II) ions, the

hydrophobic model drug, coumarin 102, encapsulated in the core of micelles was released in a sustained manner due to the gradual swelling of the crosslinked core achieved by the slow penetration of Cu(II) ions.

Keywords.

Thiosemicarbazone, RAFT, Sustained drug release, Cu(II) ions, Polymer sensor

3.2 Introduction

Recently, the studies of controlled release of drugs and other medicine from polymeric devices have attracted attention of many researchers all over the world. Controlled drug delivery applied to delivery over days, weeks, months, years and target release on burst or sustained release.[1] Burst release can be defined as the initial large amount of drug is released before the release rate reaches a stable state. This phenomenon produces higher initial drug release and decreases the effective lifetime of the device.[2] Sustained drug release systems can be used to decrease the necessary amount of drug to cause the same therapeutic effect to target disease and to regulate the temporal drug profile for maximum therapeutic benefits.[3] T Higuchi reported the knowledge of controlled drug release at 1963. The sustained drug delivery demonstrated in 1966.[4] Since that time, many studies have demonstrated the efficiency approach.[5-9]

Drug delivery studies have been reported using the amphiphilic or stimuli-responsive block copolymers.[10-13] The important problem with amphiphilic or stimuli-responsive block copolymer micelles is their spontaneous dissociation at concentrations below critical micelle concentration (CMC). To solve the problem, various cross-linking methods of micellar cores or shells are effectively conducted employed to make the polymer micelle structure. JK Oh's group reported the core-cross-linked micelles (CCMs) through the

formation of disulfide cross-linkages. Further, they demonstrate reduction-responsive enhanced release of encapsulated drugs.[14] GH Hwang et al. proposed the pH-triggered release of drug-loaded polymer micelles by metal-ligand coordinated core cross-links.[15]

Recently, the selective detection and efficient separation of transition metal ions have become increasingly important. Among them, Sensing of Cu(II) ions has attracted more attention because they can have both merits and demerits on human health and the environment. In the past, Cu(II) ions have been detected by atomic absorbance spectroscopy (AAS), inductively coupled plasma (ICP), voltammetry, and *piezoelectric* effect, which are often high-cost and time-consuming methods.[16] An alternative methods for selective detection is the use of colorimetric or fluorescence spectroscopy. While numerous these methods have been used to detect Cu(II) ions, complexes of thiosemicarbazone ligand with Cu(II) ions have attracted attention cause anticancer, antiviral, anti-inflammatory agents and less side effects.[17-23]

The Cu(I) or Cu(II) ions not only acts a vital role in normal cells but also it plays terms of critical roles in cancer. Interestingly, many studies reported high concentrations of Cu ions in blood serum and breast cancer. The lymphoma, bronchogenic, reticulum cell sarcoma, and cervical, breast, stomach and also lung cancers showed high serum Cu ions concentration.[24] For example, higher serum and tissue Cu ions concentrations were

detected in breast cancer, suggesting that homeostasis of Cu ions is changed by malignancy. Certainly, Cu ions have been shown to promote cancer growth and metastasis.[24-26] Considering the increase of Cu ions by malignant cells and promotion of cancer progression, thiosemicarbazone is emerging as a potential target for developing new anti-cancer therapeutics.[27-30] we recently reported selective colorimetric sensing of Cu(II) ions with phenylthiosemicarbazone units of the polymer-based sensors in aqueous media.[16] Compared to small molecular thiosemicarbazone sensor, p(DMA-*co*-PVHC) have been used to detect Cu(II) ions and tunable sensitivity driven by pH. Furthermore, p(DMA-*co*-PVHC) with Cu(II) coordination complexes, the excellent separation of Cu(II) ions from the other metal cations by thermal precipitation, such as temperature, pH, and light.

Herein, we report a polymeric micelle colorimetric probe containing drug delivery system. In the new concept of sensing and drug delivery, the resulting p(DMA-*b*-PVHC) block copolymers produce a selective and sensitive chemosensor only to Cu(II) ions, proceeding through micellization with Coumarin 102 dyes. Cu(II) ions can be slowly penetrated into the core of micelle and act as a cross-linker of time-dependent. On the other hand, the complexes of thiosemicarbazone blocks with Cu(II) ions by coordinate interactions would render the polymers more hydrophilic, leading to increasing hydrophilicity of the hydrophobic core of pVHC blocks of p(DMA-*b*-PVHC) micelles. Besides, complexations

of thiosemicarbazone blocks with Cu(II) ions can act as the relaxing matrices for drug delivery and releases system

3.3 Experimental

3.3.1 Materials

2-(Dodecylthiocarbonothioylthio)-2-methylpropionic acid (DMP, 98%), 2,2′-azobisisobutyronitrile (AIBN, 98%), *N*,*N*-dimethylformamide (DMF, 99.8%), tetrahydrofuran (99.9%), 1,3,5-trioxane (99%), and all the metal salts with the highest purity available were purchased from Aldrich and used as received. 4-phenylthiosemicarbazide (98.0%) were purchased from TCI (Tokyo Chemical Industry) and used as received. 3-Vinylbenzaldehye (VBA, Aldrich, 97%) and *N*,*N*-dimethylacrylamide (DMA, TCI, 99.0%) were passed through a column of basic alumina before polymerization.

3.3.2 Instrumentation

^{1}H nuclear magnetic resonance (NMR, Bruker Avance 300 MHz NMR) spectroscopy was performed in $CDCl_3$. Gel permeation chromatography (GPC, Agilent technologies 1200 series) was conducted using a polystyrene standard with DMF as the eluent at 30 ^{o}C and a flow rate of 1.00 mL/min. The UV-Vis spectra were recorded using an SINCO Mega Array PDA UV-Vis spectrophotometer. Hydrodynamic size distributions were obtained by dynamic light scattering (DLS, Nano ZS, Malvern, U.K.). Fluorescence emission spectra

were recorded with a HORIBA FluoroMax-4Pmspectrophotometers. Atomic force microscope (AFM) images were obtained using NX10 AFM (Park systems, Suwon, Korea).

3.3.3 Synthesis

Poly(*N*,*N*-dimethylacrylamide) (PDMA) DMA (9.60 ml, 97.04 mmol), DMP (176.9 mg, 0.485 mmol), AIBN (1.99 mg, 0.012 mmol), 1,3,5-trioxane (43.6 mg, 0.485 mmol, internal standard), and DMF (10.0 mL) were added in a 25 mL Schlenk flask equipped with a magnetic stir bar. The solution was purged with argon for 20 min, and the reaction flask was placed in a preheated oil bath at 70 ℃. After 1 h, the polymerization was quenched by removing the polymerization from heat and exposing the solution to air. The solution was precipitated into cold ether. The polymer was redissolved in THF and reprecipitated into the cold ether and dried under vacuum at room temperature for 24 h. M_n = 21 500 g/mol, M_w/M_n = 1.06. ^{1}H NMR (300 MHz, $CDCl_3$, δ in ppm): 2.85 (6H, s, -N(C*H*$_3$)$_2$); 2.00-1.00 (3H, m, -C*H*$_2$C*H*-); 0.85 (3H, t, -C*H*$_3$)

Poly[(N,N-dimethylacrylamide)-*b*-(3-vinylbenzaldehyde)] [p(DMA-*b*-VBA)] p(DMA-*b*-VBA) block copolymer was synthesized by RAFT polymerization using PDMA as a macro chain transfer agent (macroCTA). 3-Vinylbenzaldehyde (0.164 ml, 1.29 mmol), PDMA (0.31 g, 0.026 mmol), AIBN (1.06 mg, 0.00645 mmol), 1,3,5-trioxane (23.2 mg, 0.26 mmol, internal standard), and DMF (5 mL) were sealed in a 10 mL Schlenk flask

equipped with a magnetic stir bar. The solution was purged with argon for 20 min, and the reaction flask was placed in a preheated oil bath at 70 ℃. The solution was purged with argon for 20 min, and the reaction flask was placed in a preheated oil bath at 70 ℃. After 3h, the polymerization was quenched by removing the polymerization from heat and exposing the solution to air. The solution was precipitated into cold ether. The polymer was redissolved in THF and reprecipitated into the cold ether and dried under vacuum at room temperature for 24 h. M_n = 24 400 g/mol, M_w/M_n = 1.07. ^{1}H NMR (300 MHz, $CDCl_3$, δ in ppm): 9.95 (1H, s, -C*H*O); 7.80-6.4 (4H, s, Ar*H*); 2.85 (6H, s, 2.85 (6H, s, -N(CH_3)$_2$); 2.00-1.00 (3H, m, -CH_2C*H*-); 0.85 (3H, t, -CH_3)

Poly{[N,N-dimethylacrylamide]-*b*-[N-phenyl-2-(3-vinylbenzylidene)hydrazinecarbothioamide]} [p(DMA-*b*-PVHC)] Post-polymerization modification reaction was conducted as previously reported.[16] Briefly, p(DMA-*b*-VBA) (0.179 g, 0.135 mmol per VBA repeating unit) and 4-phenylthiosemicarbazide (45.2 mg, 0.270 mmol) were added to a round-bottomed flask and dissolved in THF (50 mL) and heated at 80 ℃ overnight. The solution was concentrated and precipitated in diethyl ether. The precipitation process was repeated two times and dried in a vacuum oven at 30 ℃. M_n = 24 500 g/mol , M_w/M_n = 1.08. ^{1}H NMR (300 MHz, $CDCl_3$, δ in ppm): 9.60 (1H, s, −N*H*); 9.0 (1H, s, −N*H*); 7.80 (1H, s, −C*H*N−); 7.80−6.80 (9H, m, ArH).

3.4 Results and Discussion

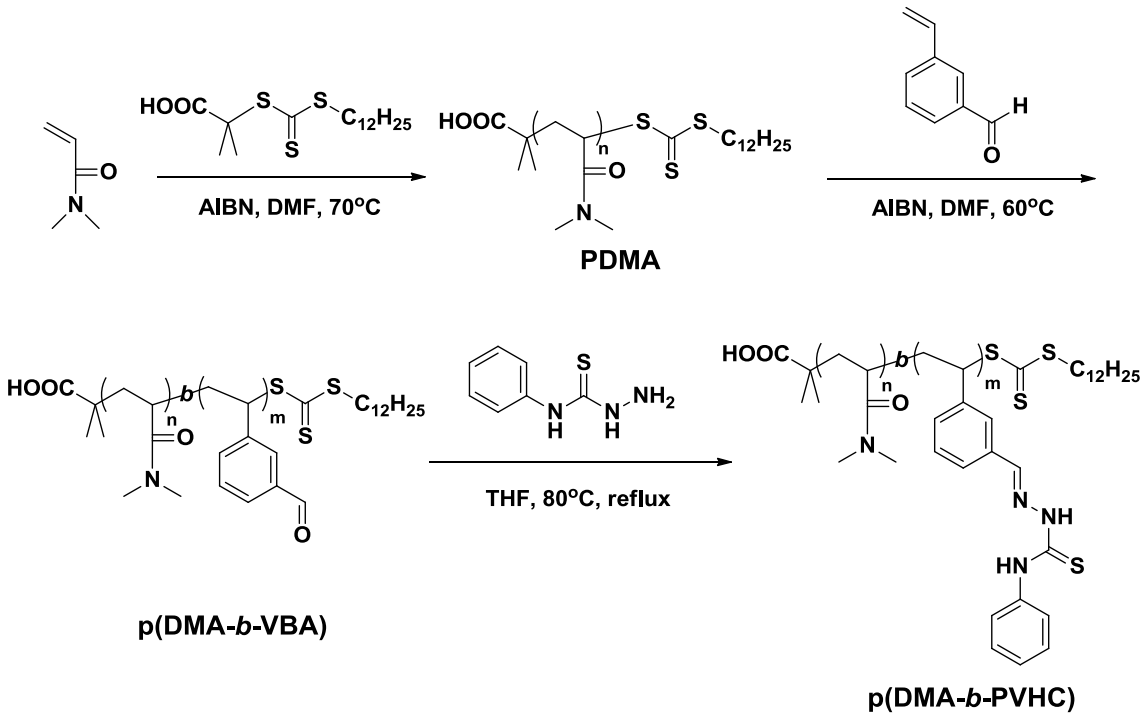

Scheme 1. Synthesis of p(DMA-*b*-VBA) via RAFT homopolymerization of DMA and subsequent RAFT block copolymerization of 3-VBA, followed by post-polymerization modification of p(DMA-*b*-VBA) to yield amphiphilic block copolymer p(DMA-*b*-PVHC) with thiocarbazone moieties.

The strategy used in this study is depicted in Scheme 1. RAFT polymerization of DMA with DMP as a chain transfer agent (CTA) and AIBN as an initiator led to PDMA with a well-controlled molecular weight and narrow polydispersity. Polymerization was carried out with [DMA]:[DMP]:[AIBN] = 200:1:0.025 in the presence of 1,3,5-trioxane as an internal standard at 70 ^{o}C. Polymerization was quenched when the monomer conversion of

DMA reached 60 % in 1h. The apparent molecular weight ($M_{n,\ app}$ = 21,500) with narrow molecular weight distribution (M_w/M_n = 1.06) of the resulting PDMA were obtained by GPC (Figure 1). Apparent molecular weight obtained by GPC was higher than the theoretical molecular weight ($M_{n,\ theory}$ = 12,200, $DP_{n,\ theory}$ = 120) calculated from the conversion of DMA. Experimental molecular weight can be also determined by ^{1}H NMR spectroscopy. $M_{n,\ NMR}$ was determined from the integration of dimethyl signals of DMA repeating units at 2.85 ppm and the signals at 0.85 ppm of the DMP end groups (-CH_3). $M_{n,\ NMR}$ (11,800 g/mol) was in relatively good agreement with $M_{n,\ theory}$ (Figure 2a).

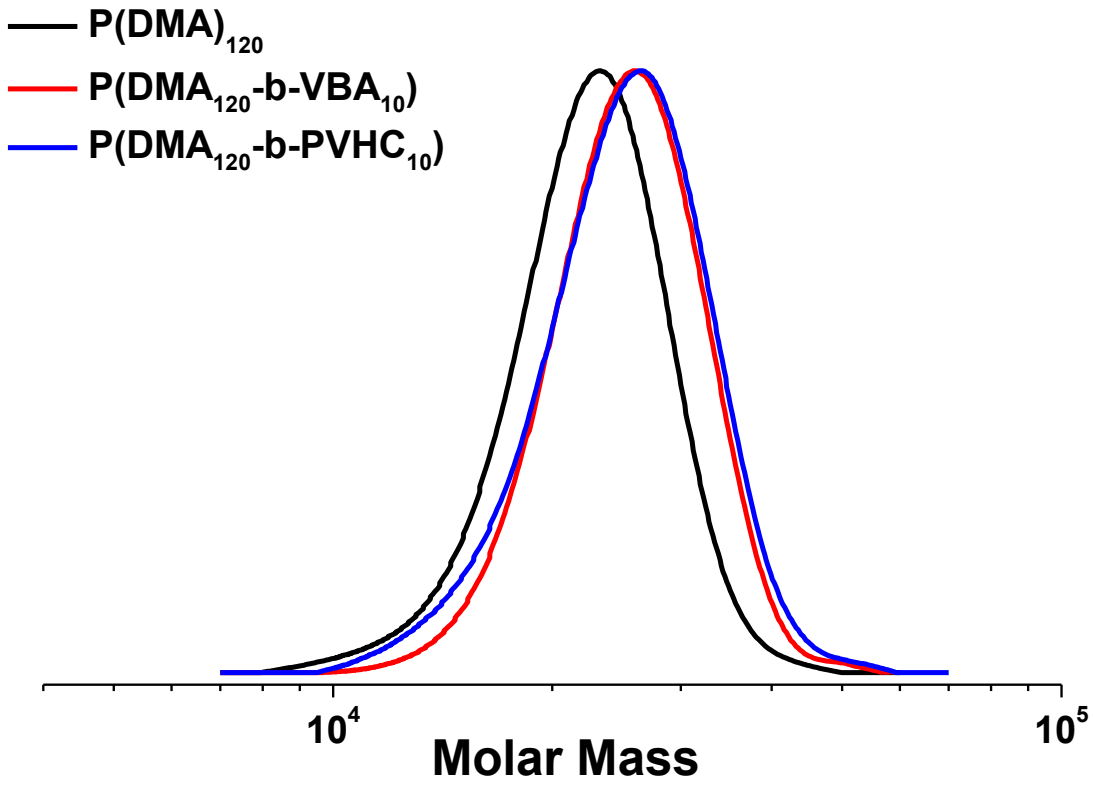

Figure 1. Overlaid GPC traces of PDMA, p(DMA-*b*-VBA), and p(DMA-*b*-PVHC).

Table 1. Results from the synthesis of PDMA, p(DMA-*b*-VBA), and p(DMA-*b*-PVHC) via RAFT polymerization, followed by postpolymerization modification

Polymer	Conv[a] (%)	$M_{n,\ theory}$[b]	$M_{n,\ NMR}$[c]	$M_{n,\ app}$[d]	PDI[d]
$P(DMA)_{120}$	60	11 800	12 200	21 500	1.06
$P(DMA_{120}$-*b*-$VBA_{10})$	20	13 100	14 600	24 400	1.07
$P(DMA_{120}$-*b*-$PVHC_{10})$	-	-	15 000	24 500	1.08

[a] Monomer conversion determined by ^{1}H NMR spectroscopy. [b] Theoretical molecular weight determined by monomer conversions. [c] Experimental molecular weight calculated from ^{1}H NMR spectroscopy. [d] Apparent number-average molecular weight and PDI determined by DMF GPC with PMMA calibration.

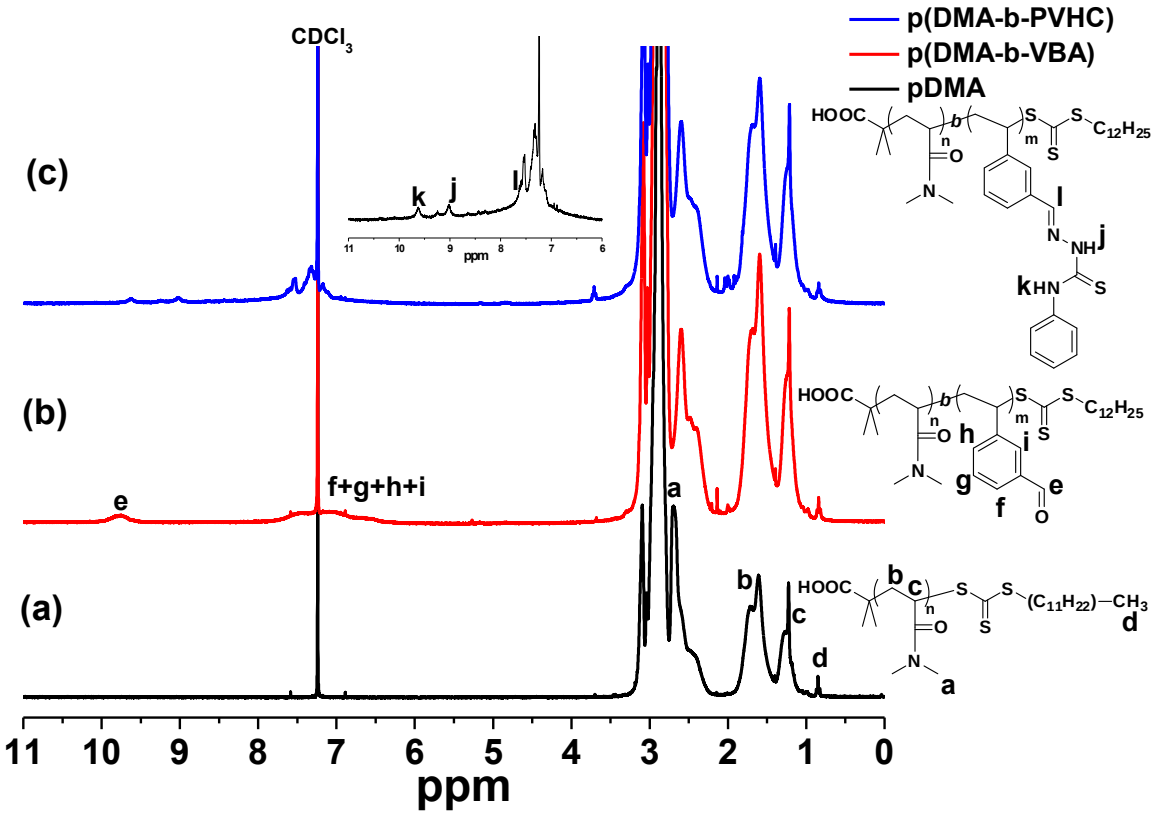

Figure 2. ^{1}H NMR spectra of PDMA, p(DMA-*b*-VBA), and p(DMA-*b*-PVHC).

RAFT polymerization of VBA was initiated with the well-defined pDMA macroCTA. The polymerization was performed in DMF and the ratio of [VBA]:[PDMA mcaroCTA]:[AIBN] was fixed at 50:1:0.25. VBA conversion was 15% in 3h, resulting in p(DMA-*b*-VBA) block copolymer (M_n = 13,100 and M_w/M_n = 1.07). The increase in the molecular weight of p(DMA-*b*-VBA) is demonstrated by the slight shift of the GPC traces toward higher molecular weight while the molecular weight distribution remained relatively low, showing the effective control over the block copolymerization (Figure 1 and Table 1). The experimental molecular weight of p(DMA-*b*-VBA) were also obtained from ^{1}H NMR spectroscopy by calculating the integration area of the DMA repeat unit signals at 2.85 ppm (-N(CH_3)$_2$) and the signal of the VBA repeat unit (-C*H*O) at 9.95 ppm ($M_{n,\ NMR}$ = 13,500, where DP_{NMR} of DMA and VBA is 120 and 10, respectively) (Figure 2b).

Having obtained the p(DMA-*b*-VBA) block copolymer, post-modification reaction was conducted to yield p(DMA-*b*-PVHC) with thiocarbazone moieties. 4-Phenylsemithiocarbazide was successfully coupled to p(DMA-*b*-VBA) with high efficiency. To ensure full conversion, a two-fold excess amount of 4-phenylsemithiocarbazide over aldehyde groups of VBA block in p(DMA-*b*-VBA) was used at 80 ℃ for 12h. ^{1}H NMR spectroscopic analysis confirmed the successful transformation of p(DMA-*b*-VBA) to p(DMA-*b*-PVHC). New peaks (i, j, k) of p(DMA-*b*-PVHC)

appeared at approximately 7.8-10.0 ppm while an aldehyde peak (e) of p(DMA-*b*-VBA) disappeared completely. The reaction was almost quantitative, with essentially complete conversion of the aldehyde units being observed. The GPC traces showed that there was no significant change in the apparent molecular weight after the coupling reaction (Figure 1).

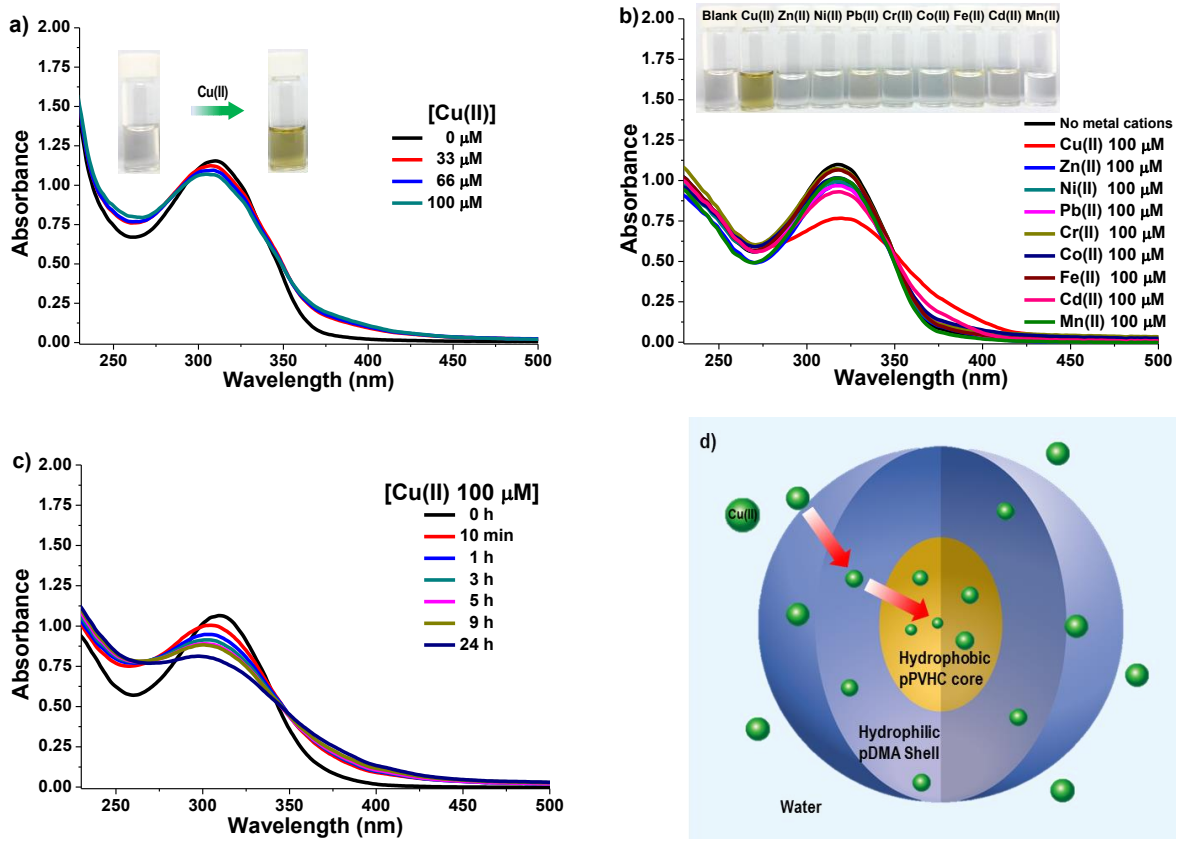

Figure 3. a) UV-Vis absorption spectra of 0.1 mg/mL p(DMA-*b*-PVHC) micellar solution (66 μM of the phenylthiosemicarbazone units) obtained right after the addition of various concentrations of Cu(II) ions in an aqueous solution at room temperature. b) Selectivity of p(DMA-*b*-PVHC) micelles with various metal ions. c) Time-dependent change in UV-Vis absorption spectra of 0.1 mg/mL p(DMA-*b*-PVHC) micellar solution with the addition of 100 μM of Cu(II) ions. d) Schematic representation of the time-dependent detection of Cu(II) ions due to their slow penetration into a hydrophobic PVHC core.

p(DMA-*b*-PVHC) block copolymer is amphiphilic and can self-assemble into micelles in aqueous solution. The critical micelle concentration (CMC) value is an important characteristic of a surfactant. The CMC value of p(DMA-*b*-PVHC) copolymer was detected using a fluorescence technique with pyrene as a probe, and calculated to be 6.6×10^{-3} mg/mL (Figure S1).

The Cu(II) ion sensing studies with self-assembled micelles of p(DMA-*b*-PVHC) were carried out in aqueous solution. An aqueous micellar solution (0.1 mg/mL) of p(DMA-*b*-PVHC) was prepared in a 66 μM concentration of phenylthiosemicarbazone units. To ensure the successful formation of micelles, p(DMA-*b*-PVHC) was micellized at a much higher concentration than CMC. Changes in UV-Vis absorption spectral responses of p(DMA-*b*-PVHC) micelles were monitored upon the gradual addition of Cu(II) ions in the concentration range of 33-100 μM (Figure 3a). The gradual decrease in the absorption maximum at 318 nm and the gradual increase in absorbance at 390 nm with the overall broadening of the absorption band were observed. The original colorless solution became yellow with the addition of Cu(II) ions due to the formation of coordination complexes between Cu(II) ions and phenylthiosemicarbazone units of p(DMA-*b*-PVHC) micelles.[16, 31] As previously reported, p(DMA-*b*-PVHC) exhibited good selectivity toward Cu(II) ions over several alkalies and transition metal cations (Figure 2b). Interestingly, this detection

process is time-dependent. Changes in UV-Vis absorption spectral responses of p(DMA-*b*-PVHC) micelles with time elapse were monitored in 100 μM of Cu(II) ions (Figure 3c and see also Figure S2a and S2b for different concentrations of Cu(II) ions). It was found that time required for the complete detection of Cu(II) ions with p(DMA-*b*-PVHC) micelles was about 24 h. The detection time profile of p(DMA-*b*-PVHC) micelles toward Cu(II) ions at different concentrations was plotted to show time-dependent detection progress (Figure S2c). The hydrophilic Cu(II) ions have limited access to the inner core of the micelles where pPVHC blocks with phenylthiosemicarbazone receptor units are closely packed. As time progressed, Cu(II) ions slowly penetrated into a hydrophobic pPVHC core and caused the time-dependent formation of coordination complexes (Figure 3d).

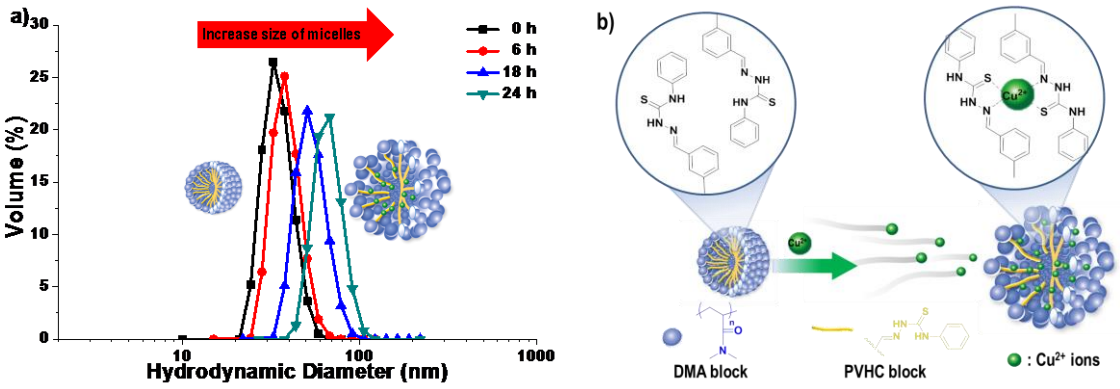

Figure 4. a) Time-dependent increase in apparent hydrodynamic diameters of 0.01 mg/mL p(DMA-*b*-PVHC) micellar solution after the addition of 100 μM of Cu(II) ions. b) The formation of core crosslinked p(DMA-*b*-PVHC) micelles with ionic cores via the intermolecular tetradentate coordination complexation between Cu(II) ions and

phenylthiosemicarbazone ligand.

DLS was conducted to observe the formation of p(DMA-*b*-PVHC) micelles and change in size of micelles resulting from Cu(II) detection via the formation of coordination complexes. For this, 100 μM of Cu(II) ions was added to the 0.01 mg/mL of p(DMA-*b*-PVHC) micellar solution in water and the evolution of size distributions were measured as time progressed (Figure 4a). The average hydrodynamic diameter of original micelles was 40 nm, indicating that p(DMA-*b*-PVHC) self-assembled to form micellar aggregates. After the addition of 100 μM of Cu(II) ions, the average hydrodynamic diameter increased gradually with time and reached 75 nm after 24 h. It was reported that Cu(II) tends to form bidentate coordination complexes with phenylthiosemicarbazone.[17, 31] However, the formation of tetradentate coordination complexes is facilitated for p(DMA-*b*-PVHC) micelles because phenylthiosemicarbazone ligands are densely located in the inner core of micelles. The time-dependent slow penetration of Cu(II) ions into the core of micelles led to the intermolecular tetradentate coordination complexation with phenylthiosemicarbazone ligands, inducing the formation of the polymer micelles with cross-linked ionic cores (Figure 4b). As a result, the average hydrodynamic diameter increased gradually with time due to the swelling of crosslinked ionic cores in water.

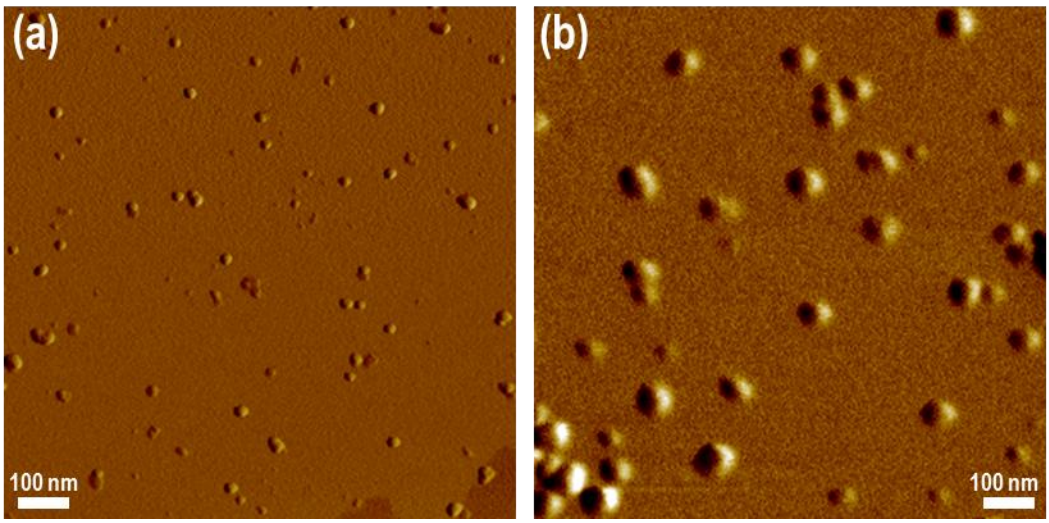

Figure 5. Representative AFM phase images of 0.01 mg/mL p(DMA-*b*-PVHC) micellar solution spin-coated on mica a) before and b) after the addition of 10 μM of Cu(II) ions.

The Cu(II) detection-induced formation of core crosslinked p(DMA-*b*-PVHC) micelles was confirmed by AFM. The samples were prepared from an aqueous solution of p(DMA-*b*-PVHC) micelles (0.01 mg/mL) and deposited directly on mica substrate by spin-coating after micellization. The uniform, well-dispersed individual spherical micelles with an average diameter of 35 nm were visualized in AFM images (Figure 5a). 10 μM of Cu(II) ions was then added to the p(DMA-*b*-PVHC) micelle solution (0.01 mg/mL) and spin-coated onto a mica substrate 24 h later for AFM analysis. While the characteristic micellar morphology was retained, the average diameter of the globular particles increased to 83 nm (Figure 5b). The core of p(DMA-*b*-PVHC) micelles were crosslinked via Cu(II) detection, rendering the resulting particles swollen.

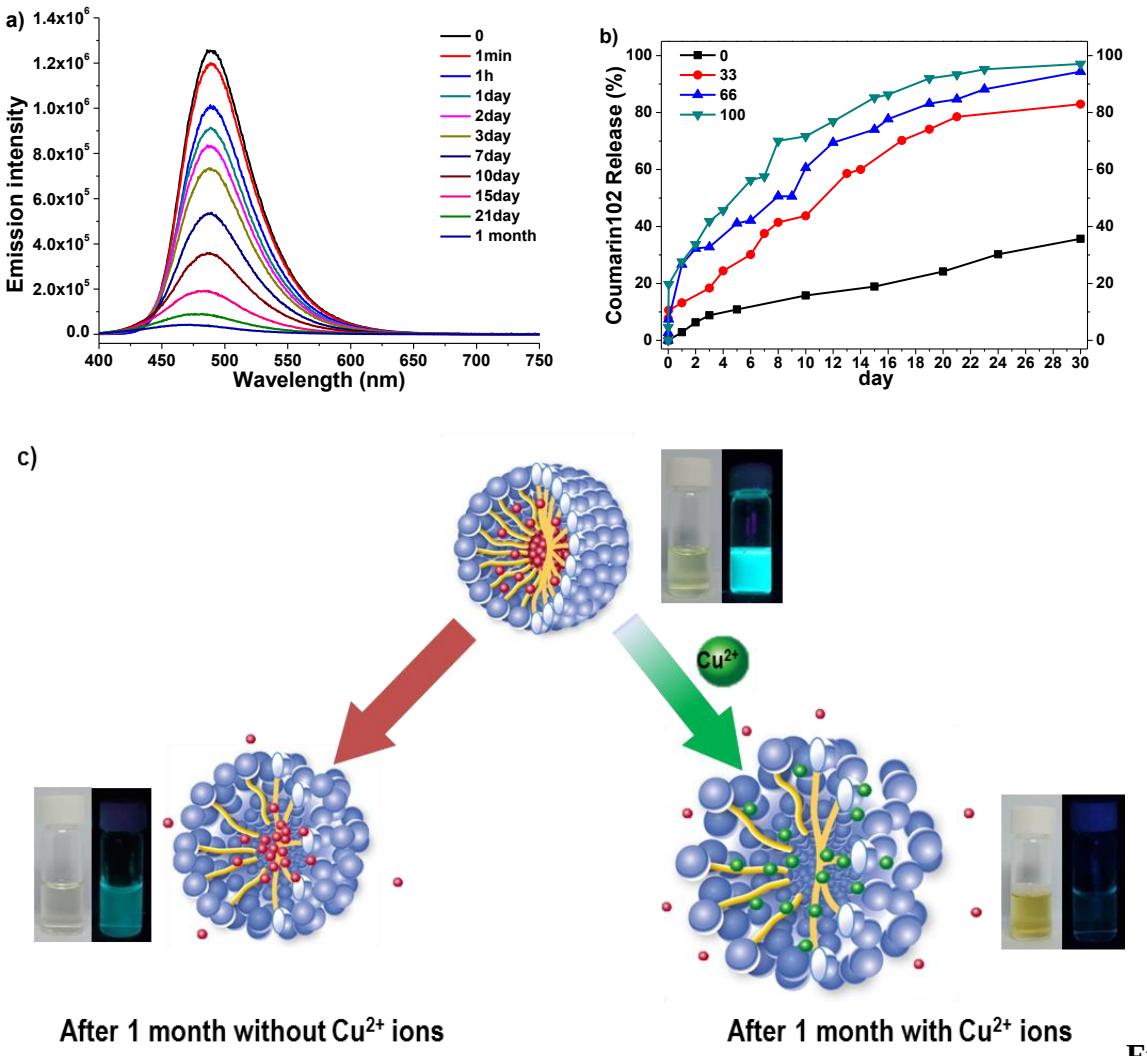

Figure 6. a) Emission spectra of an aqueous 0.1 mg/mL p(DMA-*b*-PVHC) micellar solution with encapsulated coumarin 102 after the addition of 100 μM of Cu(II) ions; the time-dependent reduction in fluorescence intensity of coumarin 102. b) The time-dependent Coumarin 102 release profiles with the addition of different concentrations Cu(II) ions obtained from normalized fluorescence intensities based on the emission maximum of each curve in spectra. c) Encapsulated dyes within the hydrophobic core of p(DMA-*b*-PVHC) micelles right after micellization (top), 35% of dye leakage after 1 month in the

absence of Cu(II) ions (left), and the complete release of encapsulated dyes after 1 month in the presence of 100 μM of Cu(II) ions (right). Each photograph of the left and right vial was taken under ambient and UV light (365 nm), respectively.

Having examined the swelling behaviors of core crosslinked p(DMA-*b*-PVHC) micelles induced by the detection of Cu(II) ions, we attempted to evaluate the effect of the gradual Cu(II)-detection on the sustained release of the hydrophobic model drug, coumarin 102. For incorporation of coumarin 102 into the core of p(DMA-*b*-PVHC) micelles, 3.0 mg of p(DMA-*b*-PVHC) and 1.0 mg of coumarin 102 were dissolved in 1 ml of THF followed by dropwise addition of 30 mL of water for 12 h. The Cu(II)-induced sustained release of encapsulated coumarin 102 was studied by fluorescence spectroscopy. The initial micellar solution exhibited the strong emission of coumarin 102 with a maximum at 490 nm. After the addition of 100 μM of Cu(II) ions, the emission intensity of coumarin 102 decreased steadily as time progressed. Approximately 7.5 and 25 % of coumarin 102 was released in 1 h and 1 day, respectively (Figure 6a). Interestingly, the amount of dye released gradually increased in a sustained manner up to 1 month with about 97% of dye being released. The release kinetics were further investigated with the different concentration of Cu(II) ions (33 and 66 μM) in parallel with a control experiment in which no Cu(II) ions were added (Figure 6b). The amount of released dye was less than 3 % in 1 day and increased up to

35% in 1 month in the absence of Cu(II) ions. This level of leakage of a hydrophobic dye from polymeric micelles in water is viable, suggesting the moderate stability of p(DMA-*b*-PVHC) micelles. When 33 or 66 μM of Cu(II) ions were added, slow release of the encapsulated coumarin 102 in comparison to the addition of 100 μM of Cu(II) ions was exhibited. The release kinetics, however, still followed a sustained fashion. The bright fluorescence was observed in the photograph of the initial colorless p(DMA-*b*-PVHC) micellar solution with coumarin 102 encapsulated. 1 month later, the solution was still colorless with a diminished fluorescence intensity due to the leakage of encapsulated coumarin 102 from polymeric micelles. This result reflects 35% of dye release obtained by fluorescence spectroscopy. After the addition of 100 μM of Cu(II) ions, however, the original colorless solution became yellow with no fluorescence intensity, indicating that almost quantitative release was achieved. While it took one day to complete the detection of Cu(II) ions followed by full swelling of core crosslinked p(DMA-*b*-PVHC) micelles, the sustained release of the encapsulated dye continued to 1 month. Though we cannot be fully certain of this prolonged release behavior, it is reasonable to assume that, unlike a burst release driven by a disruption of micelles, a diffusion-controlled release from a crosslinked swollen core requires more time.

3.5 Conclusions

Well-defined amphiphilic block copolymer, p(DMA-*b*-PVHC), was successfully synthesized using RAFT polymerization, followed by post-polymerization modification with 4-phenylthiosemicarbazide. The sensing of Cu(II) ions in aqueous media described here rely on the slow penetration of Cu(II) ions into the hydrophobic core of PVHC blocks of p(DMA-*b*-PVHC) micelles. DLS and AFM investigations revealed that the size of micelles increased after the addition of Cu(II) ions due to the swelling of crosslinked ionic cores generated by the detection of Cu(II) ions. The sustained release of the hydrophobic model drug was achieved by virtue of slow swelling of core crosslinked p(DMA-*b*-PVHC) micelles. Overall, the ability of p(DMA-*b*-PVHC) micelles to detect Cu(II) ions selectively, combined with the drug release in a sustained manner, suggests significant promise in the development of potential therapeutic vehicles capable of diagnosis.

.

3.6 Supplementary information

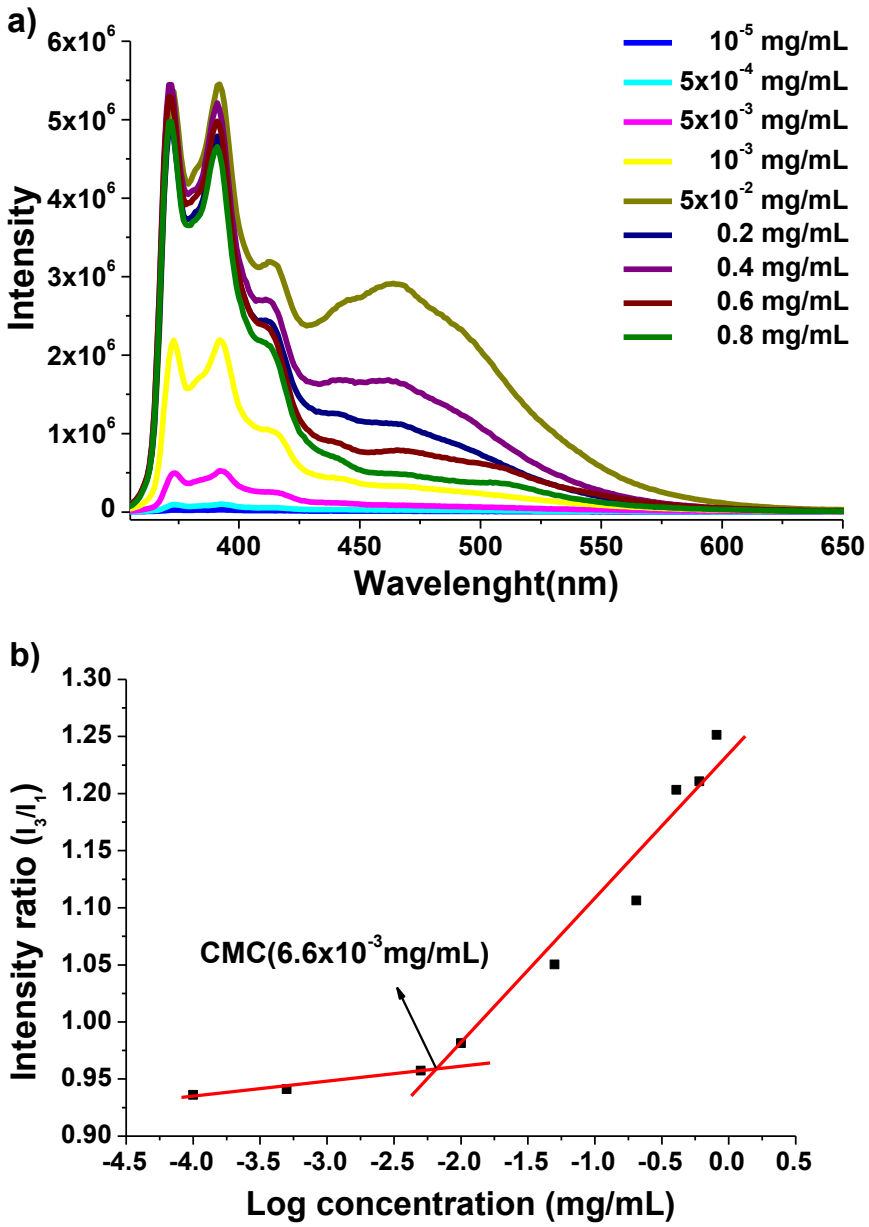

Figure S1. (a) The fluorescence emission spectra of pyrene as a function of copolymer concentration in water (mg/mL). (b) The fluorescence intensity ratio of I_{391}/I_{371} from pyrene emission spectra versus the log of the concentration (log*C*; mg/mL), a measurement used to determine the CMC for p(DMA-*b*-PVHC).

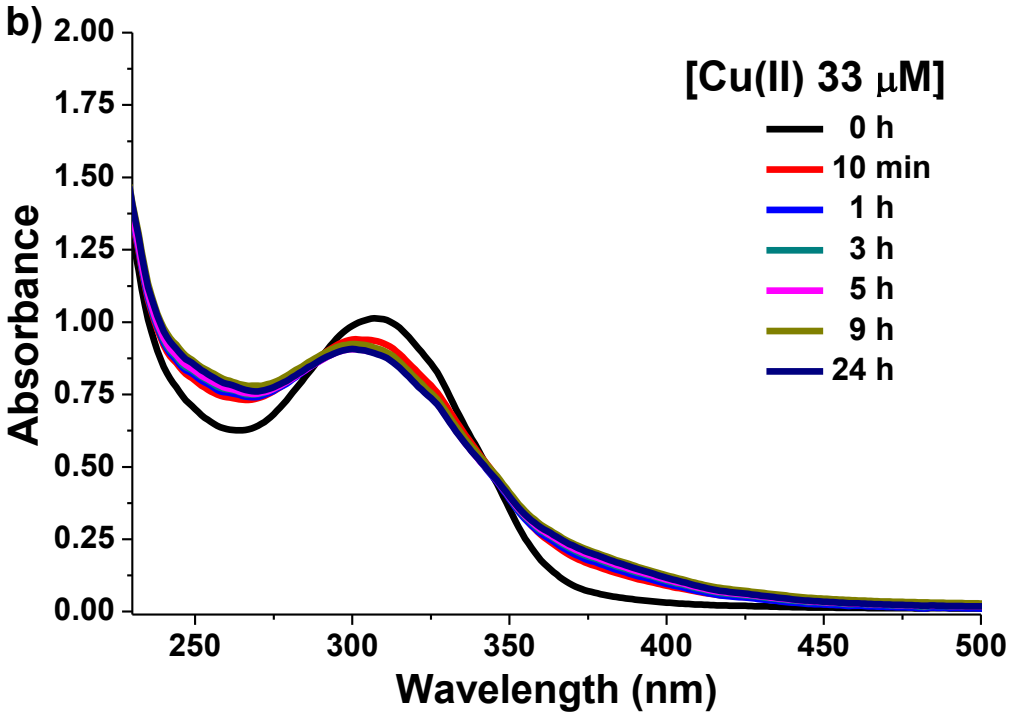
b)
[Cu(II) 33 μM]
0 h
10 min
1 h
3 h
5 h
9 h
24 h
Absorbance
Wavelength (nm)
2.00
1.75
1.50
1.25
1.00
0.75
0.50
0.25
0.00
250
300
350
400
450
500

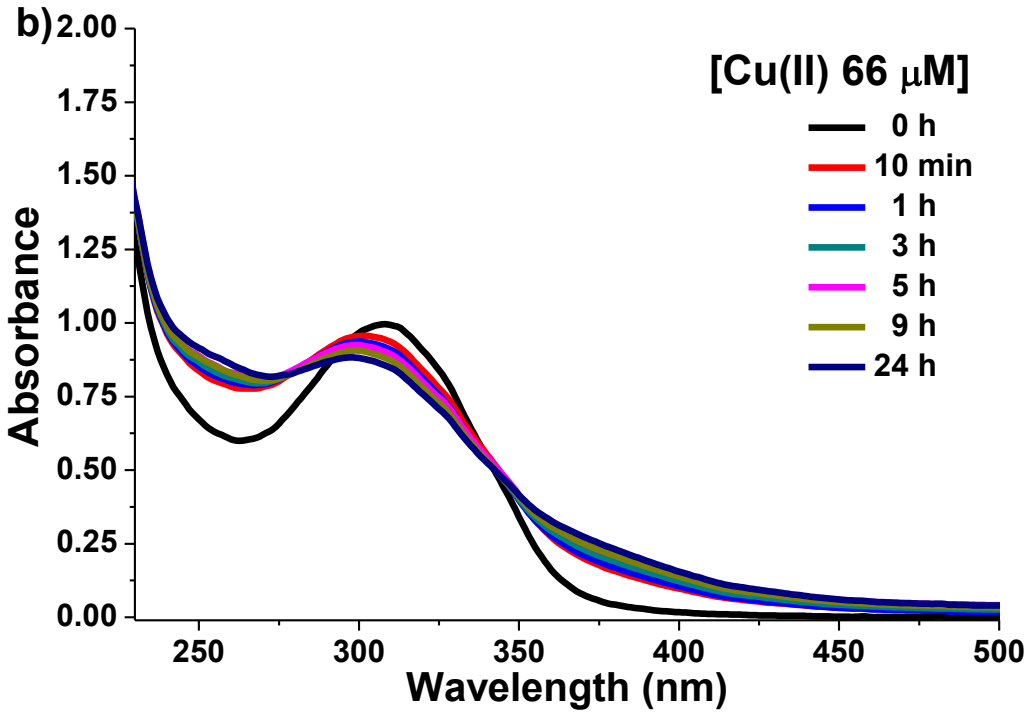
b)
[Cu(II) 66 μM]
0 h
10 min
1 h
3 h
5 h
9 h
24 h
Absorbance
Wavelength (nm)
2.00
1.75
1.50
1.25
1.00
0.75
0.50
0.25
0.00
250
300
350
400
450
500

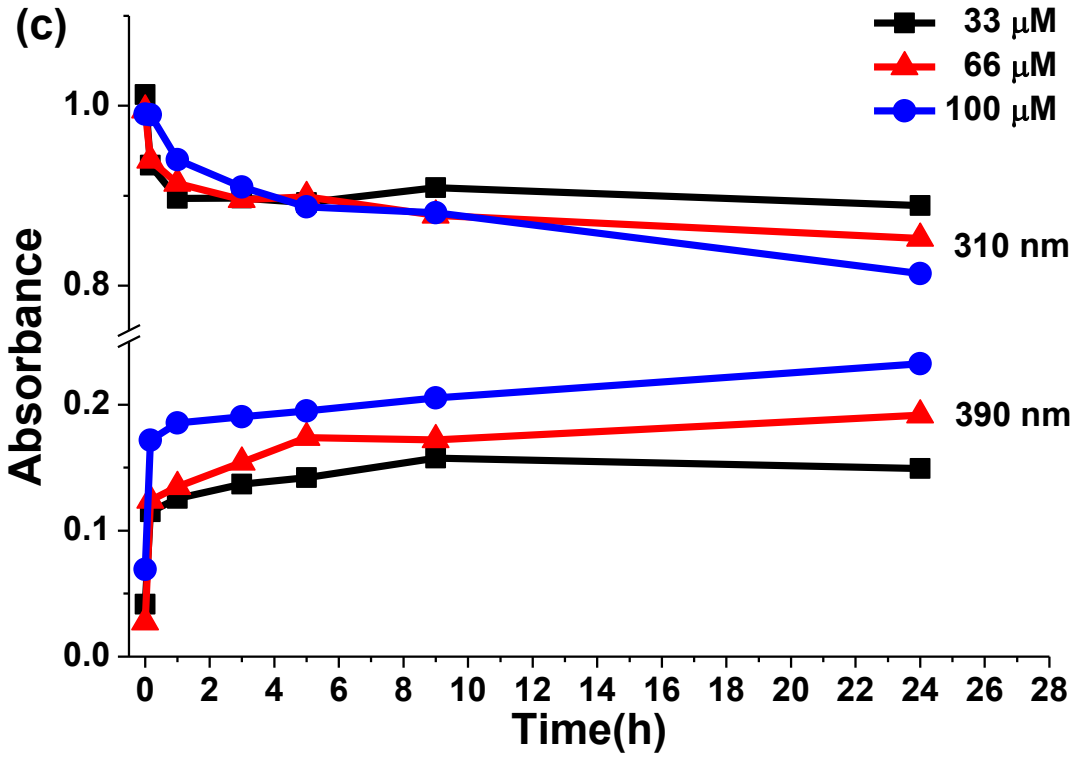

Figure S2. Time-dependent change in UV-Vis absorption spectra of 0.1 mg/mL p(DMA-*b*-PVHC) micellar solution with the addition of a) 33 μM, b) 66 μM of Cu(II) ions. C) Time-dependent change absorbance at 310 and 390 nm versus the amount of Cu(II) added.

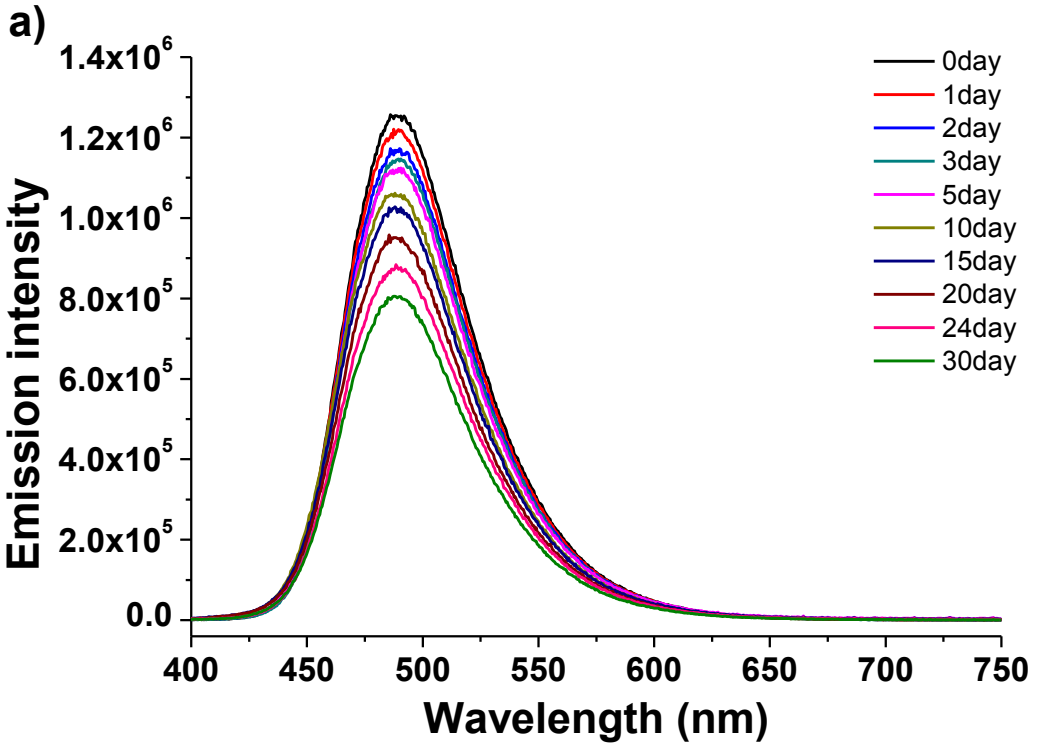
a)
Emission intensity
1.4x10^6
1.2x10^6
1.0x10^6
8.0x10^5
6.0x10^5
4.0x10^5
2.0x10^5
0.0
400
450
500
550
600
650
700
750
Wavelength (nm)
0day
1day
2day
3day
5day
10day
15day
20day
24day
30day

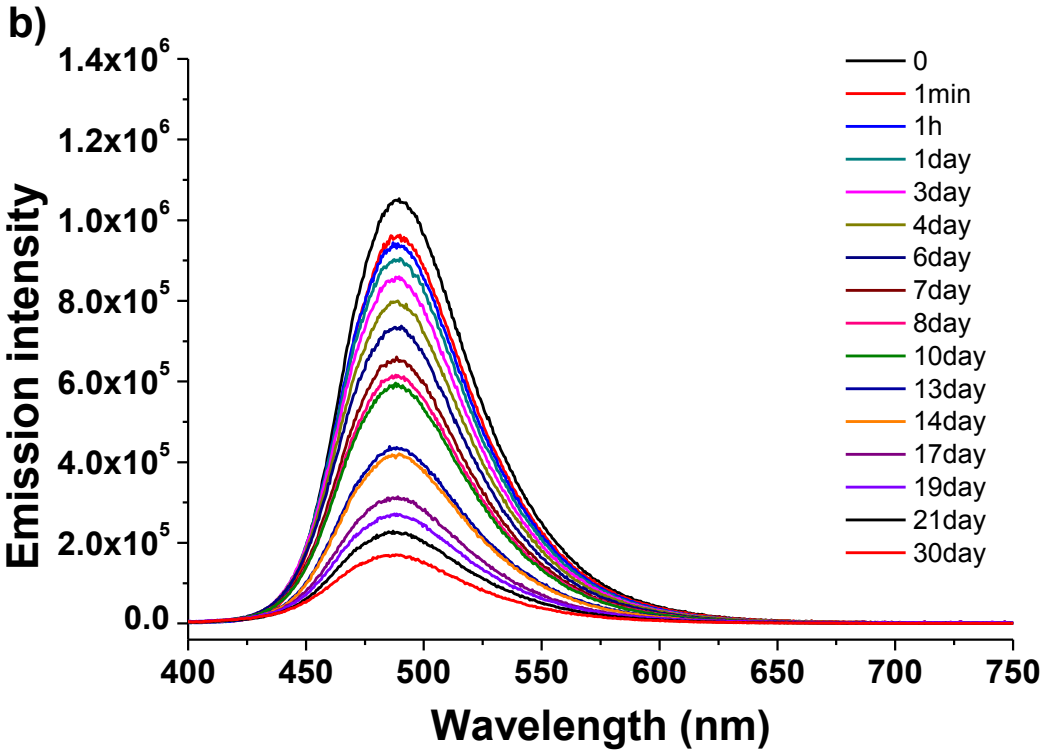
b)
Emission intensity
1.4x10^6
1.2x10^6
1.0x10^6
8.0x10^5
6.0x10^5
4.0x10^5
2.0x10^5
0.0
400
450
500
550
600
650
700
750
Wavelength (nm)
0
1min
1h
1day
3day
4day
6day
7day
8day
10day
13day
14day
17day
19day
21day
30day

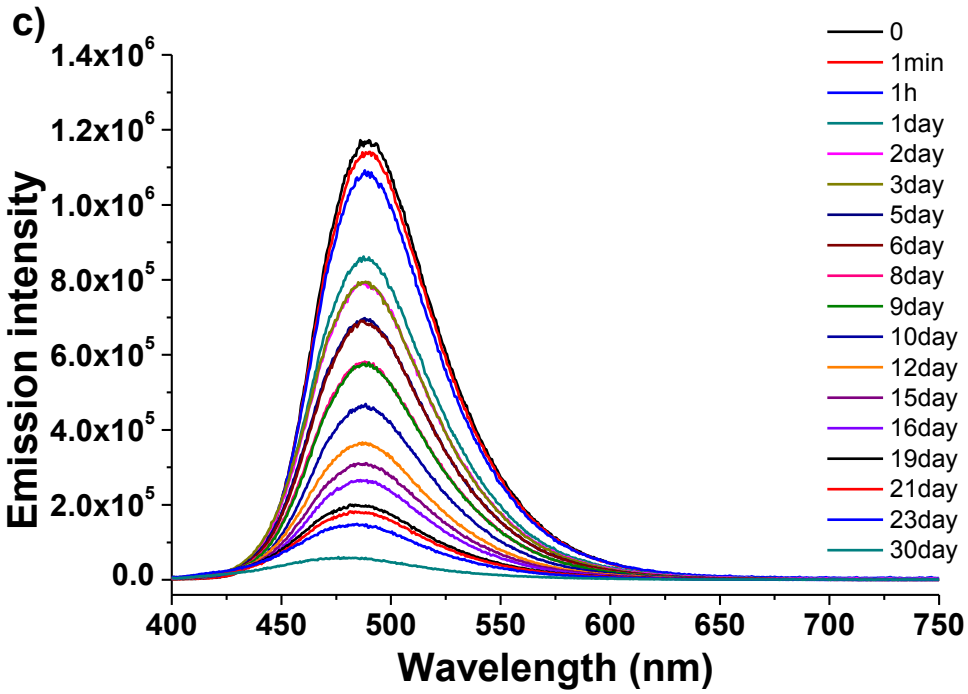

Figure S3. Emission spectra of an aqueous 0.1 mg/mL p(DMA-*b*-PVHC) micellar solution with encapsulated coumarin 102 after the addition of a) 0 μM, b) 33 μM, and 66 μM of Cu(II) ions.

3.7 References

1. Hu, J.; Liu, S. Responsive Polymers for Detection and Sensing Applications: Current Status and Future Developments. *Macromolecules* **2010,** 43 (20), 8315-8330 DOI: 10.1021/ma1005815.
2. Huang, X.; Brazel, C. S. On the importance and mechanisms of burst release in matrix-controlled drug delivery systems. *Journal of controlled release* **2001,** 73 (2-3), 121-136.
3. Uhrich, K. E.; Cannizzaro, S. M.; Langer, R. S.; Shakesheff, K. M. Polymeric Systems for Controlled Drug Release. *Chemical Reviews* **1999,** 99 (11), 3181-3198 DOI: 10.1021/cr940351u.
4. Folkman, J.; Long, D. M.; Rosenbaum, R. Silicone rubber: a new diffusion property useful for general anesthesia. *Science* **1966,** 154 (3745), 148-149.
5. Lee, S. S.; Hughes, P.; Ross, A. D.; Robinson, M. R. Biodegradable implants for sustained drug release in the eye. *Pharmaceutical research* **2010,** 27 (10), 2043-53 DOI: 10.1007/s11095-010-0159-x.
6. Arora, S.; Ali, J.; Ahuja, A.; Khar, R. K.; Baboota, S. Floating drug delivery systems: a review. *Aaps PharmSciTech* **2005,** 6 (3), E372-E390.
7. Zhu, Y.; Shi, J.; Shen, W.; Dong, X.; Feng, J.; Ruan, M.; Li, Y. Stimuli-Responsive Controlled Drug Release from a Hollow Mesoporous Silica Sphere/Polyelectrolyte Multilayer Core-Shell Structure. *Angewandte Chemie* **2005,** 117 (32), 5213-5217 DOI: 10.1002/ange.200501500.
8. Gultepe, E.; Nagesha, D.; Sridhar, S.; Amiji, M. Nanoporous inorganic membranes or coatings for sustained drug delivery in implantable devices. *Advanced drug delivery reviews* **2010,** 62 (3), 305-15 DOI: 10.1016/j.addr.2009.11.003.
9. Carvalho, I. M.; Marques, C. S.; Oliveira, R. S.; Coelho, P. B.; Costa, P. C.; Ferreira, D. C. Sustained drug release by contact lenses for glaucoma treatment-a review. *Journal of controlled release : official journal of the Controlled Release Society* **2015,** 202, 76-82 DOI: 10.1016/j.jconrel.2015.01.023.
10. Kim, H.; Lee, H.-i. pH-responsive polymeric micelles from sulfamate-conjugated block copolymers. *Macromolecular Research* **2014,** 23 (2), 129-133 DOI: 10.1007/s13233-015-3013-5.
11. Lee, J.-E.; Ahn, E.; Bak, J. M.; Jung, S.-H.; Park, J. M.; Kim, B.-S.; Lee, H.-i. Polymeric micelles based on photocleavable linkers tethered with a model drug. *Polymer* **2014,** 55 (6), 1436-1442 DOI: 10.1016/j.polymer.2014.01.026.

12. Bak, J. M.; Lee, H.-i. Novel thermoresponsive fluorinated double-hydrophilic poly{[N-(2,2-difluoroethyl)acrylamide]-b-[N-(2-fluoroethyl)acrylamide]} block copolymers. *Journal of Polymer Science Part A: Polymer Chemistry* **2013,** 51 (9), 1976-1982 DOI: 10.1002/pola.26578.

13. Lee, H. I.; Wu, W.; Oh, J. K.; Mueller, L.; Sherwood, G.; Peteanu, L.; Kowalewski, T.; Matyjaszewski, K. Light-induced reversible formation of polymeric micelles. *Angew Chem Int Ed Engl* **2007,** 46 (14), 2453-7 DOI: 10.1002/anie.200604278.

14. Biswas, D.; An, S. Y.; Li, Y.; Wang, X.; Oh, J. K. Intracellular Delivery of Colloidally Stable Core-Cross-Linked Triblock Copolymer Micelles with Glutathione-Responsive Enhanced Drug Release for Cancer Therapy. *Molecular pharmaceutics* **2017,** 14 (8), 2518-2528 DOI: 10.1021/acs.molpharmaceut.6b01146.

15. Hwang, G. H.; Min, K. H.; Lee, H. J.; Nam, H. Y.; Choi, G. H.; Kim, B. J.; Jeong, S. Y.; Lee, S. C. pH-responsive robust polymer micelles with metal-ligand coordinated core cross-links. *Chemical communications* **2014,** 50 (33), 4351-3 DOI: 10.1039/c4cc01584c.

16. Bak, J. M.; Lee, H.-i. Water-Soluble Polymeric Probe for the Selective Sensing and Separation of Cu(II) Ions in Aqueous Media: pH-Tunable Detection Sensitivity and Efficient Separation by Thermal Precipitation. *Macromolecules* **2017,** 50 (21), 8529-8535 DOI: 10.1021/acs.macromol.7b02066.

17. Park, K. C.; Fouani, L.; Jansson, P. J.; Wooi, D.; Sahni, S.; Lane, D. J.; Palanimuthu, D.; Lok, H. C.; Kovacevic, Z.; Huang, M. L.; Kalinowski, D. S.; Richardson, D. R. Copper and conquer: copper complexes of di-2-pyridylketone thiosemicarbazones as novel anti-cancer therapeutics. *Metallomics : integrated biometal science* **2016,** 8 (9), 874-86 DOI: 10.1039/c6mt00105j.

18. Richardson, D. R.; Kalinowski, D. S.; Richardson, V.; Sharpe, P. C.; Lovejoy, D. B.; Islam, M.; Bernhardt, P. V. 2-Acetylpyridine thiosemicarbazones are potent iron chelators and antiproliferative agents: redox activity, iron complexation and characterization of their antitumor activity. *Journal of medicinal chemistry* **2009,** 52 (5), 1459-1470.

19. Richardson, D. R.; Sharpe, P. C.; Lovejoy, D. B.; Senaratne, D.; Kalinowski, D. S.; Islam, M.; Bernhardt, P. V. Dipyridyl thiosemicarbazone chelators with potent and selective antitumor activity form iron complexes with redox activity. *Journal of medicinal chemistry* **2006,** 49 (22), 6510-6521.

20. Afrasiabi, Z. Transition metal complexes of phenanthrenequinone thiosemicarbazone as potential anticancer agents: synthesis, structure, spectroscopy, electrochemistry and in vitro anticancer activity against human breast cancer cell-line,

T47D. *Journal of Inorganic Biochemistry* **2003,** 95 (4), 306-314 DOI: 10.1016/s0162-0134(03)00131-4.

21. Abid, M.; Azam, A. Synthesis and antiamoebic activities of 1-N-substituted cyclised pyrazoline analogues of thiosemicarbazones. *Bioorganic & medicinal chemistry* **2005,** 13 (6), 2213-20 DOI: 10.1016/j.bmc.2004.12.050.

22. Hameed, A.; Khan, K. M.; Zehra, S. T.; Ahmed, R.; Shafiq, Z.; Bakht, S. M.; Yaqub, M.; Hussain, M.; de la Vega de Leon, A.; Furtmann, N.; Bajorath, J.; Shad, H. A.; Tahir, M. N.; Iqbal, J. Synthesis, biological evaluation and molecular docking of N-phenyl thiosemicarbazones as urease inhibitors. *Bioorganic chemistry* **2015,** 61, 51-7 DOI: 10.1016/j.bioorg.2015.06.004.

23. Popiołek, Ł.; Paruch, K.; Patrejko, P.; Biernasiuk, A.; Wujec, M. New 3-hydroxy-2-naphthoic hydrazide derivatives: thiosemicarbazides and 1,2,4-triazole-3-thiones, their synthesis and in vitro antimicrobial evaluation. *Journal of the Iranian Chemical Society* **2016,** 13 (10), 1945-1951 DOI: 10.1007/s13738-016-0911-1.

24. Kuo, H. W.; Chen, S. F.; Wu, C. C.; Chen, D. R.; Lee, J. H. Serum and tissue trace elements in patients with breast cancer in Taiwan. *Biological Trace Element Research* **2002,** 89 (1), 1-11.

25. Gupte, A.; Mumper, R. J. Elevated copper and oxidative stress in cancer cells as a target for cancer treatment. *Cancer treatment reviews* **2009,** 35 (1), 32-46.

26. Brem, S. S.; Zagzag, D.; Tsanaclis, A.; Gately, S.; Elkouby, M.; Brien, S. Inhibition of angiogenesis and tumor growth in the brain. Suppression of endothelial cell turnover by penicillamine and the depletion of copper, an angiogenic cofactor. *The American journal of pathology* **1990,** 137 (5), 1121.

27. Denoyer, D.; Masaldan, S.; La Fontaine, S.; Cater, M. A. Targeting copper in cancer therapy:'Copper That Cancer'. *Metallomics : integrated biometal science* **2015,** 7 (11), 1459-1476.

28. Kalinowski, D. S.; Stefani, C.; Toyokuni, S.; Ganz, T.; Anderson, G. J.; Subramaniam, N. V.; Trinder, D.; Olynyk, J. K.; Chua, A.; Jansson, P. J. Redox cycling metals: Pedaling their roles in metabolism and their use in the development of novel therapeutics. *Biochimica et Biophysica Acta (BBA)-Molecular Cell Research* **2016,** 1863 (4), 727-748.

29. Lovejoy, D. B.; Jansson, P. J.; Brunk, U. T.; Wong, J.; Ponka, P.; Richardson, D. R. Antitumor activity of metal-chelating compound Dp44mT is mediated by formation of a redox-active copper complex that accumulates in lysosomes. *Cancer research* **2011,** 71 (17), 5871-5880.

30. Jansson, P. J.; Yamagishi, T.; Arvind, A.; Seebacher, N.; Gutierrez, E.; Stacy, A.; Maleki, S.; Sharp, D.; Sahni, S.; Richardson, D. R. Di-2-pyridylketone 4, 4-Dimethyl-3-thiosemicarbazone (Dp44mT) Overcomes Multidrug-Resistance by a Novel Mechanism Involving the Hijacking of Lysosomal P-Glycoprotein (Pgp). *Journal of Biological Chemistry* **2015**, jbc. M114. 631283.

31. Udhayakumari, D.; Velmathi, S.; Chen, W.-C.; Wu, S.-P. A dual-mode chemosensor: Highly selective colorimetric fluorescent probe for Cu2+ and F− ions. *Sensors and Actuators B: Chemical* **2014,** 204, 375-381 DOI: 10.1016/j.snb.2014.07.109.